

Annual high-resolution grazing intensity maps on the Qinghai-Tibet Plateau from 1990 to 2020

Jia Zhou^{1,2}, Jin Niu³, Ning Wu¹, Tao Lu^{1*}

¹Chengdu Institute of Biology, Chinese Academy of Sciences, Chengdu 610213041, China

²University of Chinese Academy of Sciences, Beijing 100049, China

³Department of Economics, Brown University, Providence, 02912, USA

Correspondence to: Tao Lu (lutao@cib.ac.cn)

Abstract. Grazing activities constitute the paramount challenge to grassland conservation over the Qinghai-Tibet Plateau (QTP), underscoring the urgency for obtaining detailed extent, patterns, and trends of grazing information to access efficient grassland management and sustainable development. Here, to inform these issues, we provided the first annual Gridded Dataset of Grazing Intensity maps (GDGI) with a resolution of 100 meters from 1990 to 2020 for the QTP. Five most commonly used machine learning algorithms were leveraged to develop livestock spatialization model, which spatially disaggregate the livestock census data at the county level into a detailed 100 m× 100 m grid, based on seven key predictors from terrain, climate, vegetation and socio-economic factors. Among these algorithms, the extreme trees (ET) model performed the best in representing the complex nonlinear relationship between various environmental factors and livestock intensity, with an average absolute error of just 0.081 SU/hm², a rate outperforming the other models by 21.58%–414.60%. By using the ET model, we further generated the GDGI dataset for the QTP to reveal the spatio-temporal heterogeneity and variation in grazing intensities. The GDGI indicates grazing intensity remained high and largely stable from 1990 to 1997, followed by a sharp decline from 1997 to 2001, and fluctuated thereafter. Encouragingly, comparing with other open-access datasets for grazing distribution on the QTP, the GDGI has the highest accuracy, with the determinant coefficient (R^2) exceed 0.8. Given its high resolution, recentness and robustness, we believe that the GDGI dataset can significantly enhance understanding of the substantial threats to grasslands emanating from overgrazing activities. Furthermore, the GDGI product holds considerable potential as a foundational source for other researches, facilitating rational utilization of grasslands, refined environmental impact assessments, and the sustainable development of animal husbandry. The GDGI product developed in this study is available at <https://doi.org/10.5281/zenodo.13141090><https://doi.org/10.5281/zenodo.10851119> (Zhou et al., 2024).

31 **1 Introduction**

32 Livestock is a crucial contributor to global food systems through the provision of essential animal
33 proteins and fats, and plays a significant role in supporting human survival and socio-economic
34 development (Gilbert et al., 2018; Godfray et al., 2018; Humpenöder et al., 2022; Kumar et al., 2022).
35 However, the escalating increase in human demand for meat and dairy products over recent decades has
36 triggered a livestock boom, which in turn has increasingly threatened grassland ecosystems and placed
37 a heavy burden on the environment through overgrazing and land-use change (Tabassum et al., 2016;
38 Wei et al., 2022; Minoofar et al., 2023). It is estimated that up to 300 million hectares of land are used
39 globally for grazing and cultivating fodder crops (Tabassum et al., 2016). Grazing activities could alter
40 vegetation phenology and community structure (Dong et al., 2020), and trigger deforestation (García
41 Ruiz et al., 2020), grassland degradation (Sun et al., 2020), soil erosion (Shakoor et al., 2021), and
42 associated direct releases in greenhouse gas that lead to climate change feedback (Godfray et al., 2018;
43 Chang et al., 2021). Additionally, livestock are responsible for large-scale dispersion of pathogens,
44 organic matter, and residual medications into soil and groundwater, thereby contaminating the
45 environment (Venglovsky et al., 2009; Tabassum et al., 2016; Hu et al., 2017; Muloi et al., 2022).
46 Consequently, more and more scholars have called attention to provide reliable contemporary dataset to
47 illustrate the spatio-temporal heterogeneity and variation of livestock (Petz et al., 2014; Fetzel et al.,
48 2017; Zhang et al., 2018; Li et al., 2021).

49 One of the major challenges in monitoring grazing activity at regional or even larger scale, is the
50 determination of the livestock distribution pattern. Despite the importance of geographical grazing
51 information, high spatio-temporal grazing dataset remain unavailable, posing the most critical challenge
52 to grassland management, particularly for vulnerable grassland ecosystems in fragile regions grappling
53 with economic and sustainable development contradictions (Meng et al., 2023; Pozo et al., 2021; Miao et
54 al., 2020; He et al., 2022). In the early 2000s, the Food and Agriculture Organization of the United
55 Nations (FAO) launched the Gridded Livestock of the World (GLW) project to facilitate a detailed
56 evaluation of livestock production, aiming to provide pixel-scale livestock densities instead of traditional
57 administrative unit benchmarks (Nicolas et al., 2016). Consequently, the world's inaugural dataset of
58 livestock spatialization map (GLW1) was released in 2007, providing the first globally standardized
59 livestock density distribution map at a spatial resolution of 0.05 decimal degrees (≈ 5 km at the equator)
60 for 2002. It was not until 2014 that an updated GLW2 map with a 1 km resolution for 2006 was
61 released, by using a stratified regression approach, superior spatial resolution predictor variables, and
62 more detailed livestock census data (Robinson et al., 2014). Furthermore, an evolutionary step in
63 machine learning technology saw Gilbert et al. (2018) using random forests algorithm to forge a global
64 livestock distribution map with a 10-km resolution for 2010 (GLW3), succeeding traditional multivariate
65 regression methods and surpassing the precision of previous GLW1 and GLW2 maps. Beyond these
66 global mappings, several maps with different scales have also been published, including intercontinental,
67 national, state or provincial, and local scale (Neumann et al., 2009; Prosser et al., 2011; Van Boeckel et
68 al., 2011; Nicolas et al., 2016). However, these maps are fundamentally coarse due to constraints such as
69 the availability of fine scale and contemporary census data, the grazing spatialization method, as well as
70 the identification of appropriate indicators, thereby limiting their application to local or regional-scale
71 studies (Nicolas et al., 2016; Gilbert et al., 2018; Robinson et al., 2014). Hence, there is an emergent

72 demand for more refined grazing map products (Mulligan et al., 2020; Martinuzzi et al., 2021).

73 An exemplar of this need can be observed in the Qinghai-Tibet Plateau (QTP), the world's most
74 elevated pastoral region and an important grazing area in China (Zhan et al., 2023). It was possessing
75 abundant grassland that spans 1.5 million km², accounting for 50.43% of China's total grassland area,
76 with Yak and Tibetan sheep as primary grazing livestock (Feng et al., 2009; Cai et al., 2014; Zhan et al.,
77 2023). Over recent decades, the QTP has undergone escalating grassland degradation, leading to many
78 ecological and socio-economic problems, which calls for an urgent need for detailed livestock
79 distribution dataset (Li et al., 2022a). Unfortunately, despite researchers' efforts at mapping the QTP's
80 grazing intensity, current livestock dataset still suffer from coarse spatio-temporal resolution and
81 modelling accuracy. Apart from the aforementioned global grazing dataset, several other maps also
82 cover the QTP. For instance, Liu et al. (2021) generated annual 250-m gridded carrying capacity maps
83 for 2000-2019, by employing multiple linear regressions of livestock numbers, population density, NPP,
84 and topographic features. Li et al. (2021) used machine learning algorithms to produce gridded livestock
85 distribution data at 1 km resolution for 2000-2015 in western China at five year interval, based on
86 county-level livestock census data and 13 factors from land use practice, topography, climate, and
87 socioeconomic aspects, including grassland coverage, arable land coverage, forest land coverage, desert
88 coverage, NDVI, elevation, slope, daytime surface temperature, precipitation, distance to river, travel
89 time to major cities, population density, and GDP (Li et al., 2021). A contribution from Meng et al.
90 (2023) brought forth annual longer time-series grazing maps by using random forests model, integrating
91 climate, soil, NDVI, water distance, and settlement density to decompose county-level livestock census
92 data to a 0.083° (≈10 km at the equator) grid for 1982-2015 (Meng et al., 2023). Similarly, Zhan et al.
93 (2023) also used random forests algorithm to combine eleven influence factors to provide a winter and
94 summer grazing density map at 500 m resolution for 2020 (Zhan et al., 2023).

95 However, although these maps have provided good help in understanding grazing conditions on the
96 QTP, there are currently still no maps that can satisfy the need for fine-scale grassland management
97 with a long time span. In addition, the available livestock distribution maps of the QTP still need
98 improvement in terms of modelling techniques and factor selection to obtain high-precision livestock
99 spatialization data. For example, traditional methods like multiple linear regression, while proven
100 fundamental and widely applicable for livestock spatialization (Robinson et al., 2014; Ma et al., 2022),
101 are being challenged by the development of computational science in recent years. Among them,
102 machine learning technology is providing new opportunities towards more accurate predictions of
103 livestock distribution (García et al., 2020). Random forests regression, for instance, is currently widely
104 used to construct global, national as well as regional livestock spatialization dataset, and has been proved
105 to have much better accuracy than traditional mapping techniques (Rokach, 2016; Nicolas et al., 2016;
106 Gilbert et al., 2018; Dara et al., 2020; Chen et al., 2019; Li et al., 2021). Nevertheless, other more
107 advanced machine learning methods with superior feature learning and more robust generalization
108 capabilities, remains largely untapped for modelling geographic data (Ahmad et al., 2018; Heddam et al.,
109 2020; Long et al., 2022). Thus, exploring the potential application of new advanced machine learning
110 technologies in livestock spatialization remains a critical task. Furthermore, selecting the suitable factors
111 that influencing livestock grazing preferences is also the other critical challenge for enhancing the
112 precision of grazing distribution dataset (Meng et al., 2023). Livestock grazing activities are often
113 affected by abiotic and biotic resources, including climatic and environmental factors (Waha et al.,
114 2018), herd foraging and grazing behaviours (Garrett et al., 2018; Miao et al., 2020), and

115 conservation-oriented policies (Li et al., 2021). For instance, regions exceeding elevations of 5,600 m or
116 slope greater than 40% are customarily unsuitable for grazing (Luo et al., 2013; Mack et al., 2013;
117 Robinson et al., 2014; Chen et al., 2019). Moreover, the livestock generally prefer areas abundant in
118 water and pasture resources for foraging (Li et al., 2021). Besides, ecological conservation policies also
119 exert substantial influence, significantly affecting grazing distribution relative to the level of
120 conservation priority. In addition, the health status of the grassland is an important factor influencing
121 whether livestock choose to feed or not (Li et al., 2021). Consequently, indicators related to the above
122 aspects are often employed to gauge the spatial heterogeneity of livestock distribution (Allred et al.,
123 2013; Sun et al., 2021; Meng et al., 2023). Nonetheless, some most commonly used indicators like NPP
124 or NDVI can result in misconceptions, as they may not fully characterize the grazing intensity. For
125 example, grasslands with high NPP or NDVI are often preferred by livestock, but this doesn't necessarily
126 correlate with grazing intensity in nature reserves due to strict policy restrictions (Veldhuis et al., 2019;
127 O'Neill and Abson, 2009; Zhang et al., 2021b). Conversely, areas with sparse grassland cover may
128 support considerable livestock numbers, despite evidence of degradation (Zhang et al., 2021a; Guo et al.,
129 2015). Accordingly, further investigation of novel indicators is imperative to enhance the correlation
130 between grassland and grazing intensity, thereby optimizing the integration of such influencing factors
131 into grazing spatialization models.

132 In summary, the QTP is in pressing need for a high spatio-temporal resolution grazing dataset to
133 address urgent and realistic challenges. But the existing livestock dataset specific to the QTP are fraught
134 with several insufficient, predominantly concerning rough resolution, relatively backward census data,
135 as well as conventional methods in livestock spatialization. Moreover, the discrepancies in predictive
136 indicators and modelling approaches within these dataset discourage their application in time-series
137 analysis. Consequently, the generation of high-resolution and high-quality grazing map products has
138 emerged as the most pressing challenge for the QTP. Here, we aim to (1) establish a methodological
139 framework by using more rational models and indicators than traditional studies to achieve fine-scale
140 livestock spatialization; (2) select the grazing spatialization model with good performance by
141 incorporating multi-source data with advanced machine learning techniques; and (3) ultimately, provide
142 an annual grazing intensity dataset with 100 m resolution spanning from 1990-2020. These maps can
143 not only provide fundamental dataset with finer spatio-temporal resolution to address the limitations of
144 existing grazing intensity maps, but enhance a better understanding of sustainable management practices
145 as well as other grassland-related issues across the QTP.

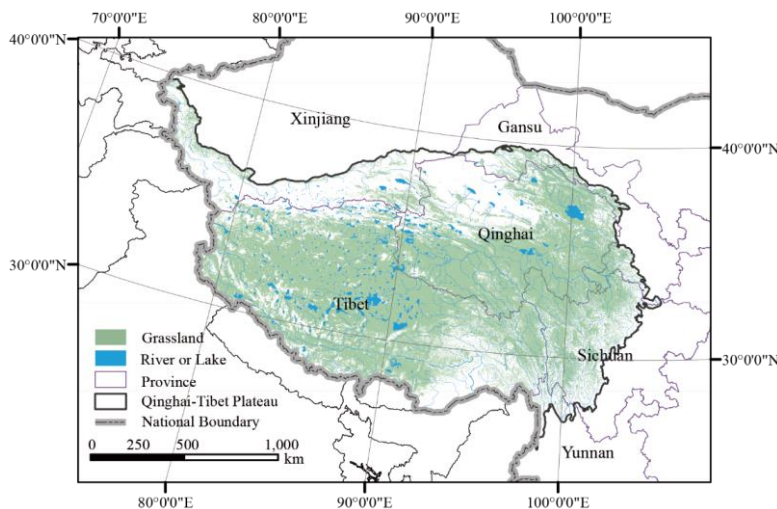
146 **2 Data and methods**

147 **2.1 Study area**

148 Known as the Asia's water tower and the world's third pole, the QTP is geographically situated
149 between 73°19'~104°47' east longitude and 26°00'~39°47' north latitude, with a total area of about 2.61
150 million square kilometers (Figure 1). Its jurisdiction encompasses 182 counties within six provincial
151 regions of China, including Tibet Autonomous Region, Qinghai Province, Xinjiang Uygur Autonomous
152 Region, Gansu Province, Sichuan Province, and Yunnan Province (Meng et al., 2023). Elevation on the
153 QTP predominantly ranges between 3,000 m and 5,000 m, with an average altitude exceeding 4,000 m.
154 With grasslands constituting over half of its land cover, the QTP emerges as one of the most important
155 pastoral areas in China. Alpine steppe, alpine meadow, and temperate steppe characterize the main
156 grassland types on the QTP (Han et al., 2019; Zhai et al., 2022; Zhu et al., 2023b). The complex

Formatted: Font: (Asian) +Body Asian (宋体), (Asian)
Chinese (Simplified, Mainland China)

157 geographical and climatic conditions of the QTP contributes to the markedly heterogeneous grassland
158 distribution, which correspondingly lead to the high heterogeneity in livestock distribution. Moreover,
159 social and economic development, coupled with policy initiatives directed towards grassland restoration,
160 have noticeably impacted the livestock numbers on the QTP over recent decades (Li et al., 2021; Li et al.,
161 2016).



162 Figure 1. The geographic zoning map of the Qinghai-Tibet Plateau (QTP) superposed with grassland vegetation.
163 Boundaries for the six provinces used for statistical analysis are also shown.

164 2.2 Data source

165 2.2.1 Census livestock data

166 The county-level census livestock data for the period between 1990 and 2020 were obtained from
167 the Bureau of Statistics of each county across the QTP (Table 1). The data includes the number of cattle,
168 sheep, horse and mule, with the exception of counties in Yunnan Province, which lack data for the
169 years from 1990 to 2007, and Ganzi Prefecture in Sichuan Province, which lack data for the years from
170 1990 to 1999, and Muli county in Sichuan Province, which lack data for the years from 1990 to 2007.
171 For these counties belonging to the same prefecture, including counties in Ganzi and Aba prefectures in
172 Sichuan Province, we used the livestock census data at the prefecture-level to carry out spatialization.
173 For these counties in Yunnan Province, since they belong to different municipalities, it is not reasonable
174 to replace them with municipal-level data. For these counties without livestock census data for some
175 years, we supplemented the missing data by linear interpolation with grazing density data in
176 available year. In total, livestock data were available for 182 counties, and 4,998 independent records
177 were finally generated. Furthermore, the respective quantities of different livestock types are converted
178 to Standard Sheep Units (SU), in compliance with the Chinese national regulations (Meng et al., 2023).

179 Due to the difficulty of collecting township-level census livestock data, the validation data at the
180 township scale collected in this study only involved these townships of Baching County (2010-2018)
181 and Gaize County (2018-2020) in Tibet, and Hongyuan County in Sichuan Province (2008). The
182 township-level census livestock data cumulatively involves 18 townships with a total of 112 records,

183 and were only used for auxiliary validation of the simulation results.

184 The validation data at the pixel scale also encompass a total of 112 records from 68 sites, which
185 were collected from literatures, questionnaires and field surveys. Specifically, 93 records at 49 sites
186 spanning the 1990-2020-2021 period were obtained from 17 literatures, 19 records at 19 sites were
187 obtained from the questionnaires and the field survey in 2021. The detailed information for these
188 records can be found in the [SupplementarySupplementary](#) files (Figure S3 and Table S3).

189 [Table 1. Summary information of the livestock data used in the modeling process study](#)

Variables	ScaleLevel	Time	Sources
	County	1990-2020	Statistical bureau
Livestock numbers	Township	2008-2020	Statistical bureau
	Pixel	1990-2021	Literatures, questionnaires and field surveys

190

191 *2.2.2 Factors affecting grazing activities*

192 [Livestock grazing activities are often affected by abiotic and biotic resources, including climatic](#)
193 [and environmental factors \(Waha et al., 2018\), herd foraging and grazing behaviours \(Garrett et al.,](#)
194 [2018; Miao et al., 2020\). For instance, high-altitude and steep hillsides are unsuitable for grazing due to](#)
195 [terrain constraints, and the distribution of herders directly affects the grazing areas \(Luo et al., 2013;](#)
196 [Mack et al., 2013; Robinson et al., 2014; Chen et al., 2019\). Moreover, the livestock generally prefer](#)
197 [areas abundant in water and pasture resources for foraging \(Li et al., 2021\). –Therefore, in this In this](#)
198 [study, topography, climatic, environmental and socio-economic impacts were considered as influential](#)
199 [factors on grazing activities \(Li et al., 2021; Meng et al., 2023\).](#)

200 ~~We utilized correlation analysis and the Random Forest importance ranking tool to eliminate~~
201 ~~redundant environmental factors and determine the contribution of each factor. Ultimately, Accordingly,~~
202 ~~altitude, slope, distance to water source, population density, air temperature, precipitation and~~
203 ~~human induced impacts on NPP (HNPP) was selected as indicators (Table2). Specifically, elevation~~
204 ~~is derived from the DEM dataset accessible via the Resource and Environmental Data Cloud Platform~~
205 ~~of the Chinese Academy of Sciences (<https://www.gscloud.cn>), which also facilitated slope calculation.~~
206 ~~Rivers and lakes were obtained from the National Tibetan Plateau Data Center (<https://data.tpdc.ac.cn>),~~
207 ~~and the nearest Euclidean distance from each pixel to rivers or lakes is calculated accordingly.~~
208 ~~Meteorological elements such as daily air temperature and precipitation were downloaded from the~~
209 ~~China Meteorological Data Service Center (<http://data.cma.cn>). For the grid dataset that is not~~
210 ~~conditionally available, including population density, temperature, precipitation and HNPP, we detailed~~
211 ~~the creation process in the Supplementary file. All datasets utilized in this study were harmonized to~~
212 ~~consistent coordinate systems and resolutions (WGS 1984 Albers, 100 m).~~

- Formatted: Indent: First line: 0 ch, Space Before: 6 pt
- Formatted: Centered
- Formatted Table
- Formatted: Centered
- Formatted: Centered
- Formatted: Centered
- Formatted: Indent: First line: 0 ch, Space Before: 12 pt
- Formatted: Space Before: 12 pt

213 [Table 2. Summary information of factors affecting grazing activities on the QTP.](#)

214

Variables	Format	Period- (years)	Time Resolution	Spatial Resolution	Source
Altitude	GeoTIFF	—	—	30m	https://www.gscloud.cn
Slope	GeoTIFF	—	—	30m	https://data.tpdac.ac.cn
Water source	Shapefile	1990-2020	Annual	—	https://data.tpdac.ac.cn
Population density	GeoTIFF	1990-2020	Annual	100m	See supplementary file
Temperature	GeoTIFF	1990-2020	Annual	100m	See supplementary file
Precipitation	GeoTIFF	1990-2020	Annual	100m	See supplementary file
HNPP	GeoTIFF	1990-2020	Annual	100m	See supplementary file

215 We utilized correlation analysis and the Random Forest importance ranking tool to eliminate
 216 redundant environmental factors and determine the contribution of each factor. Ultimately, altitude,
 217 slope, distance to water source, population density, air temperature, precipitation and human-induced
 218 impacts on NPP (HNPP) was selected as indicators (Table 2). Specifically, elevation is derived from the
 219 DEM dataset accessible via the Resource and Environmental Data Cloud Platform of the Chinese
 220 Academy of Sciences (<https://www.gscloud.cn>), which also facilitated slope calculation. Rivers and
 221 lakes were obtained from the National Tibetan Plateau Data Center (<https://data.tpdac.ac.cn>), and the
 222 nearest Euclidean distance from each pixel to rivers or lakes is calculated accordingly. Meteorological
 223 elements such as daily air temperature and precipitation were downloaded from the China
 224 Meteorological Data Service Center (<http://data.cma.cn>). For the grid dataset that is not conditionally
 225 available, including population density, temperature, precipitation and HNPP, we detailed the creation
 226 process in the Supplementary file. All datasets utilized in this study were harmonized to consistent
 227 coordinate systems and resolutions (WGS 1984 Albers, 100 m).

228 ▲

229 **2.3 Methodological framework**

230 We adopted a comprehensive methodological framework for mapping high-resolution grazing
 231 intensity on the QTP. Three major steps are included to predict the distribution pattern of grazing
 232 intensity: (1) identifying factors affecting grazing ~~activities~~activities and extracting theoretical suitable
 233 areas for livestock grazing, (2) building grazing spatialization model, and (3) filtering the model and
 234 correcting the grazing map. An exhaustive explanation of each step is provided in Figure 2.

Formatted: Font: (Asian) Segoe UI, 9 pt, Pattern: Clear (White)

Formatted: Font: (Default) Times New Roman, (Asian) Segoe UI, 9 pt, Pattern: Clear (White)

Formatted: Font: (Asian) Segoe UI, 9 pt, Pattern: Clear (White)

Formatted: Indent: First line: 0 ch

Formatted: Font: Not Bold

Formatted: Centered, Space Before: 0 pt

Formatted: Centered, Space Before: 0 pt

Formatted: Space Before: 0 pt

Formatted: Font color: Text 1

Formatted: Centered, Space Before: 0 pt

Formatted: Centered, Space Before: 0 pt

Formatted: Space Before: 0 pt

Formatted: Centered, Space Before: 0 pt

Formatted: Space Before: 0 pt

Formatted: Centered, Space Before: 0 pt

Formatted: Space Before: 0 pt

Formatted: Centered, Space Before: 0 pt

Formatted: Space Before: 0 pt

Field Code Changed

Field Code Changed

Formatted: Font: (Default) +Body (Calibri), 10.5 pt

Formatted: Indent: First line: 0 ch, Space Before: 12 pt

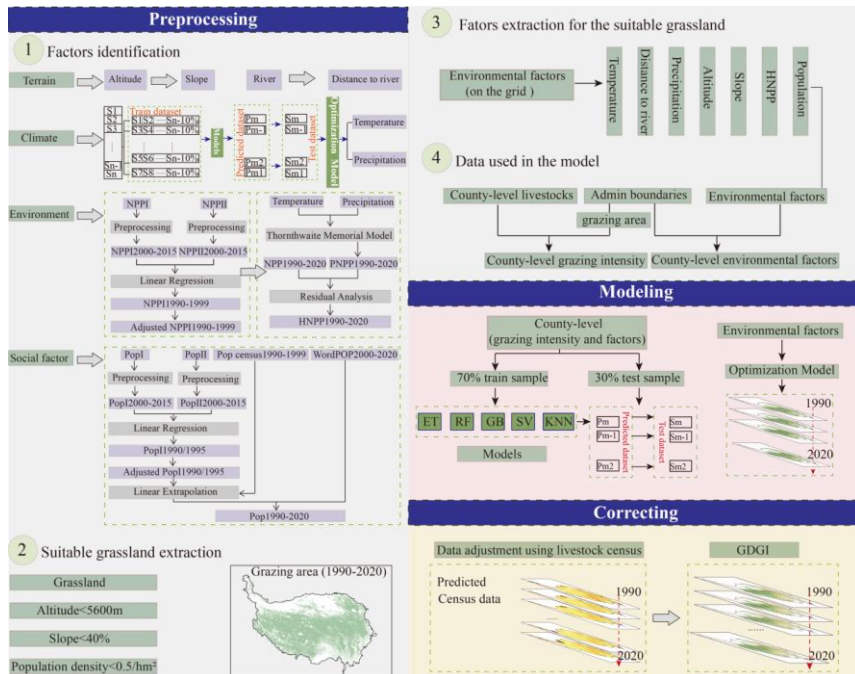


Figure 2. Flowchart of creating grazing intensity maps using different methods and source products.

235
236

237 2.3.1 Identifying factors and theoretical suitable areas for grazing

238 In this study, we assumed that grazing activities are confined solely to grassland. Consequently, the
 239 potential grazing areas for each year were identified on the basis of grassland boundaries, which was
 240 extracted from the 30 m annual land cover dataset (CLCD) (Yang and Huang, 2021). Furthermore,
 241 grassland with slope over 40% and elevation higher than 5,600 m respectively, were considered
 242 unsuitable for grazing and were therefore excluded from the potential grazing area in the subsequent
 243 simulations (Robinson et al., 2014). In addition, the grassland with population density greater than 50
 244 inhabitants km⁻² were also excluded (Li et al., 2018). The remaining isolated grassland was thus
 245 categorized as theoretical feasible grazing regions (Li et al., 2018).

246 The spatial patterns of abiotic and biotic resources, incorporating food availability, environmental
 247 stress, and herder preference critically affect grazing activities (Meng et al., 2023). In light of this,
 248 seven influencing factors in four aspects were selected for grazing intensity mapping (Figure 2-1).

249 2.3.2 Building grazing spatialization model

250 By performing regional statistics, the annual average values for each grazing influence factor were
 251 extracted from the theoretically suitable grazing areas at the county scale, and were further used as
 252 independent variables in the model construction. The dependent variable for the model was acquired by
 253 determining the livestock density within each county, followed by a logarithmic transformation of the
 254 values to normalize the distribution of the dependent variable. Consequently, a total of 4,998 samples
 255 were derived from the aforementioned independent and dependent variables. Of these samples, 70%

256 were allocated for model training, while the remaining 30% comprised the test sets, serving to validate
 257 the model's performance. Subsequently, we built grazing spatialization models using five machine
 258 learning algorithms at the county scale, including Support Vector regression (SV) (Cortes and Vapnik,
 259 1995; Lin et al., 2022), K-Nearest Neighbors (KNN) (Cover and Hart, 1967), Gradient Boosting
 260 regression (GB) (Friedman, 2001; Pan et al., 2019), Random Forests (RF) (Breiman, 2001) and Extra
 261 Trees regression (ET) (Geurts et al., 2006; Ahmad et al., 2018) (see Supplementary file for details).
 262 Lastly, to assess the accuracy of the spatialized livestock map, the predicted livestock intensity values
 263 were juxtaposed with the livestock statistical data from each respective county.

264 2.3.3 Correcting the grazing map

265 We further used the optimal model to predict the geographical distribution of grazing density across
 266 the QTP. To maintain better consistency between the predicted livestock number and the census data,
 267 the estimated results were adjusted using the census livestock numbers at the county scale as a control
 268 according to Equation (1). Consequently, the corrected and refined map is presented as the final grazing
 269 intensity map in this study.

$$270 \quad L_{correction} = \frac{L_{CCensus}}{L_{Cgrid}} \times L_{grid} \quad (1)$$

271 where $L_{correction}$ is the predicted pixel-scale livestock number after adjustment, L_{Cgrid} represents the
 272 estimated livestock number for each county, $L_{CCensus}$ is the census livestock number for each county,
 273 and L_{grid} refers to the predicted livestock number at the pixel scale.

274 2.4 Accuracy evaluation

275 We used three accuracy validation indexes to evaluate the performance of five machine learning
 276 algorithms, including coefficients of determination (R^2), mean absolute error (MAE), and root mean
 277 square error (RMSE), by through a comparison of the predicted value with the census data. The
 278 definitions of three metrics are presented in Equation (2) to (4).

$$279 \quad R^2 = 1 - \frac{\sum_{i=1}^n (C_i - P_i)^2}{\sum_{i=1}^n (C_i - \bar{C})^2} \quad (2)$$

$$280 \quad MAE = \frac{1}{n} \sum_{i=1}^n |C_i - P_i| \quad (3)$$

$$281 \quad RMSE = \sqrt{\frac{1}{n} \sum_{i=1}^n (C_i - P_i)^2} \quad (4)$$

282 where C_i and P_i are the census livestock data and the predicted value for county i , respectively; \bar{C}
 283 represents the mean census value for all county; and n gives the total number of counties.

284 2.5 uncertainties evaluation

285 Uncertainty in our grazing intensity maps can stem from multiple sources, such as the constraints of
 286 cross-scale modeling and the intrinsic inaccuracies of the input data. To quantify these uncertainties, we
 287 utilized the Monte Carlo (MC) method, conducting 100 iterations of simulation. Subsequently, we
 288 evaluated uncertainty through the Mean Relative Error (MRE) and assessed the model's robustness
 289 using the Standard Deviation (STD), following established methodologies (Yang et al., 2020;
 290 Alexander et al., 2017; Mcmillan et al., 2018)(Yang et al., 2020; Alexander et al., 2017; Memillan et al.,
 291 2018). The definitions for these metrics are delineated in Equations (5) to (7).

Formatted: Right

Uncertainty in grazing intensity map may arise from various factors, including the limitations of cross-scale models and the inherent inaccuracies of input data. To evaluate these uncertainties, we employed the Monte Carlo (MC) method, performing 100 simulations, and then assessed uncertainty using Mean Relative Error (MRE) and robustness using Standard Deviation (STD) (Yang et al., 2020; Alexander et al., 2017; Memillan et al., 2018). (Alexander et al., 2017 (McMillan, 2018 #165; Yang et al., 2020)) Their definitions are presented in Equation (5) to (7):

$$MCMG = \frac{1}{n\#} \sum_{i=1}^{n\#} f(x_i) \quad (5)$$

$$MREMRE = \frac{1}{n\#} \sum_{i=1}^{n\#} \left| \frac{x_i - \bar{x}}{\bar{x}} \right| \quad (6)$$

$$STDSTD = \frac{1}{n\#} \sum_{i=1}^{n\#} f(x_i) \sqrt{\frac{1}{n\#} \sum_{i=1}^{n\#} (x_i - \bar{x})^2} \quad (7)$$

Where x_i are random samples, $f(x_i)$ is the function evaluated at x_i , and n is the number of simulations. \bar{x} represents the mean value for all simulation maps.

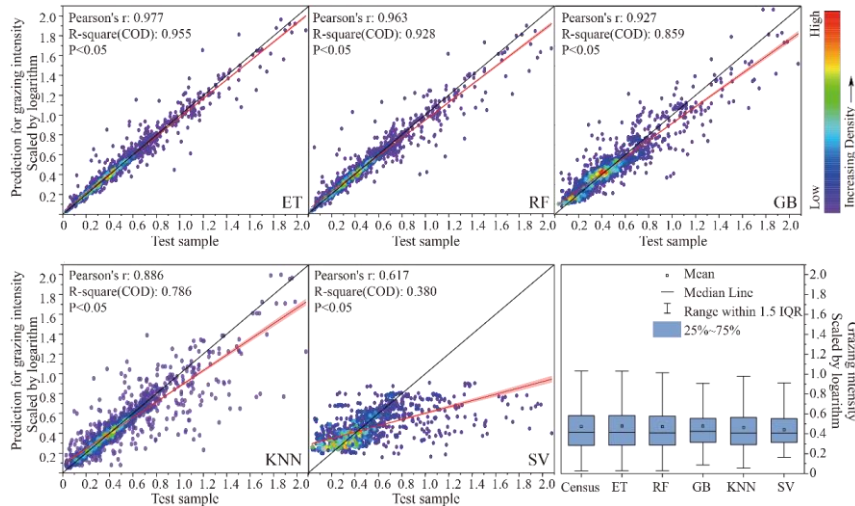
3 Results

3.1 Performances of models

Table 4.3 summarizes the efficiency of the five used machine learning models with considering all three accuracy evaluators of R^2 , MAE and RMSE. It can be seen that the ET model performs the best, with its R^2 exceeding 0.955, and MAE (0.081 SU/hm²) and RMSE (0.164 SU/hm²) significantly lower than the value of RF, GB, KNN and SVM models. Figure 3 illustrates the correlation between the census livestock data and the livestock numbers predicted by the model for each county from 1990 to 2020. It demonstrated that the ET-predicted data displayed a distribution pattern consistent with that of other models, but the scatter points of the ET model were more convergent to the 1:1 diagonal line, indicating a superior fit compared to the other models. These comparisons suggest that the ET model possesses superior robustness and can, therefore, provide stable estimations of livestock intensity on the QTP.

Table 4.3. Comparison of mapping accuracy for five machine learning models based on the same validation datasets

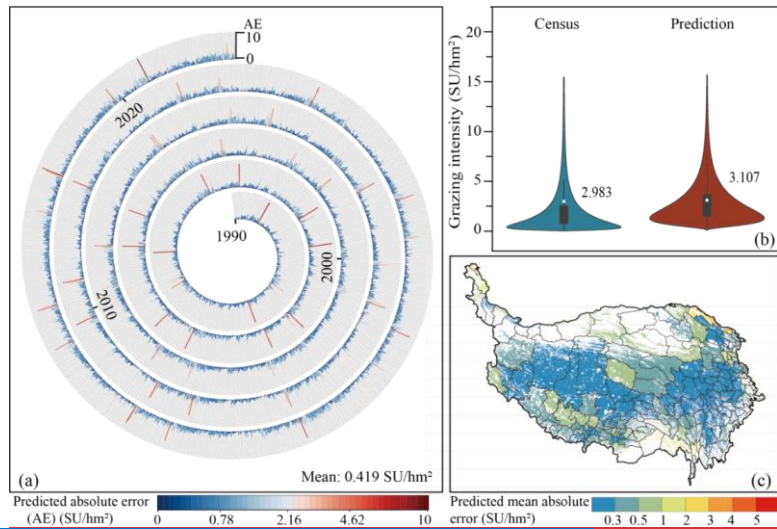
Models	R^2	MAE (SU/hm ²)	RMSE (SU/hm ²)
ET	0.955	0.081	0.164
RF	0.928	0.099	0.208
GB	0.859	0.197	0.300
KNN	0.786	0.186	0.384
SVM	0.380	0.419	0.750



318
319 Figure 3. Scatterplots of model-predicted livestock numbers and census grazing data at the county scale. The red
320 solid line and the black solid line are the fitting line and the 1:1 diagonal line, respectively.
321

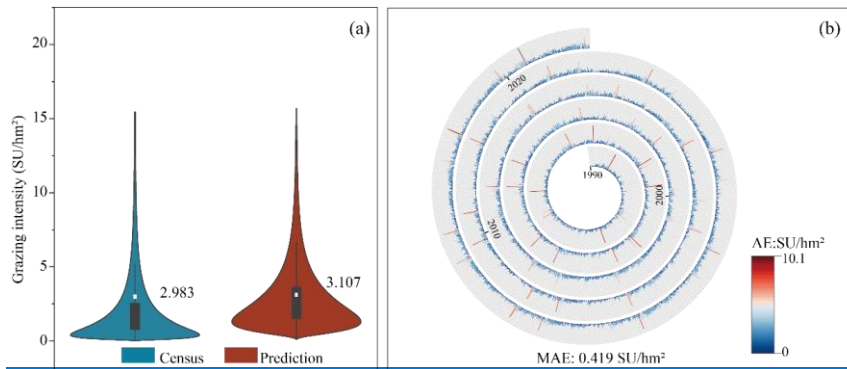
322 Utilizing the ET model, we predicted the spatio-temporal distribution of grazing intensity across the
323 QTP from 1990 to 2020 with a resolution of $100\text{ m} \times 100\text{ m}$. To test the accuracy of these maps, we
324 aggregated the prediction results from the pixel level to county level and compared them with the
325 livestock census data (Figure 4a). It is evident that the predicted livestock intensity was highly
326 consistent with the county level census data, displaying particular robustness in lower grazing intensity
327 scenarios (Figure 4b). Specifically, comparing with 2.983 SU/hm^2 for the mean census data, our
328 county-level predicted datasets revealed an average grazing intensity of 3.106 SU/hm^2 , with MAE of
329 0.123 SU/hm^2 , RMSE of 0.580 SU/hm^2 , and R^2 of 0.669 . Moreover, the data discrepancies for 76.31%
330 (number of counties=3,814) were not exceeding 0.6 SU/hm^2 , and 91.74% (number of counties=4,585)
331 remaining under 1.0 SU/hm^2 . Finally, employing county level livestock census data as a benchmark
332 for quality control, we obtained the final annual gridded datasets for grazing intensity (GDGI) across
333 the QTP spanning 31 years from 1990 to 2020.

Formatted: Font: (Asian) +Body Asian (宋体)
Formatted: Don't suppress line numbers



Formatted: Justified, Indent: First line: 1.5 ch, Space After: 0.5 line

334



335

336 Figure 4. Accuracy of the ET-predicted grazing intensity results at spatial resolution of 100 m from 1990 to 2020.

337 (a) comparison of the predicted value and the census data at the county scale from 1990 to 2020; (b) spatial

338 distribution of the mean MAE during 1990 to 2020 absolute error for each county, for each county. Figure 4.

339 Accuracy of the ET-predicted grazing intensity results at spatial resolution of 100 m from 1990 to 2020. (a)

340 absolute error (AE) between the predicted and the census data at the county scale from 1990 to 2020; (b)

341 comparison of the predicted and census data of the whole QTP from 1990 to 2020; (c) spatial distribution of the

342 mean absolute error (MAE) during 1990 to 2020 for each county.

343 Using the ET model, we projected the spatio-temporal distribution of grazing intensity across the

344 QTP from 1990 to 2020 at a 100 m × 100 m resolution. To validate the accuracy of these predictive

345 maps, we upscaled the pixel-level predictions to the county level and compared them against livestock

346 census data (Figures 4a and 4b). The results clearly show a high degree of consistency between the

347 predicted livestock intensity and the county-level census data, especially in areas with lower grazing

348 intensity (Figures 4a and 4b). Specifically, while the mean census data indicated 2.983 SU/hm² for

349 livestock intensity, our county-level predictions yielded an average of 3.106 SU/hm², with a MAE of

Formatted: Space Before: 6 pt

350 0.123 SU/hm², a RMSE of 0.580 SU/hm², and an R² value of 0.669. Additionally, 76.31% of the
351 counties (n=3,814) exhibited data discrepancies of no more than 0.6 SU/hm², and 91.74% (n=4,585)
352 had discrepancies under 1.0 SU/hm². Regarding spatial distribution, areas with data discrepancies of
353 less than 0.3 SU/hm² were predominantly located in the northwest and southeast regions of the QTP. In
354 certain counties of the northeast and southwest, the variations were even below 1.0 SU/hm² (Figure 4c).

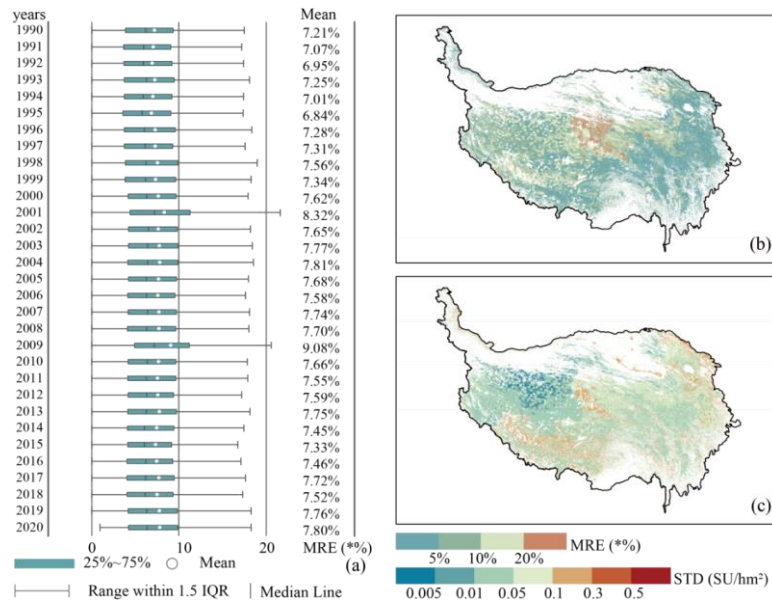
355 ▲
356

Formatted: Font color: Red

357 **3.2 uncertainties eEvaluation of uncertainties of grazing intensity map**

358 The Monte Carlo simulation results indicate that, from 1990 to 2020, the MRE in grazing intensity on the QTP,
359 based on ET method, ranged from 6.84% to 9.08% (Figure 5a). Most regions exhibited low errors; for instance, in
360 2020, areas with MRE below 5% accounted for 35.86% of the total area, and those below 10% covered 75.84%.
361 These regions were predominantly distributed in the eastern and northwestern parts of the QTP. Only 3.38% of the
362 areas had errors exceeding 20%, mainly in the southwest (Figure 5b). Robustness analysis also revealed that most
363 regions were stable. For example, in 2020, the STD was 0.059 SU/hm², with the northwestern region being
364 particularly stable, having an STD below 0.005 SU/hm². However, some fluctuations were observed in the Yarlung
365 Zangbo River basin and scattered areas in eastern Qinghai Province, but the STD remained below 0.3 SU/hm²
366 (Figure 5b). We have chosen the Mean Relative Error (MRE) as a key metric for evaluating the
367 simulation accuracy of grazing intensity within the QTP. Employing Monte Carlo simulations spanning
368 the period from 1990 to 2020, our research findings demonstrate that the average MRE for grazing
369 intensity across the QTP ranged between 6.84% and 9.08% (Figure 5a). The spatial distribution of
370 MRE indicates that the majority of the plateau exhibits low error margins. For example, in 2020, areas
371 with an MRE of less than 5% accounted for 35.86% of the total grassland area, while those with an
372 MRE below 10% constituted 75.84%. Only 3.38% of the grasslands had an MRE exceeding 20%, with
373 these regions primarily located in the southwestern portion of the QTP (Figure 5b). Moreover, the
374 robustness analysis suggests that the majority of regions within the QTP display relatively stable
375 grazing intensity trends. For instance, the overall standard deviation (STD) in 2020 was 0.059 SU/hm²,
376 with the northwest region demonstrating remarkable stability, reflected in an STD of less than 0.005
377 SU/hm². Although some areas within the Yarlung Zangbo River Basin and the eastern part of Qinghai
378 Province experienced higher variability, their STD was still maintained below 0.3 SU/hm² (Figure 5c).

Formatted: Font: 10 pt



Formatted: Centered, Indent: First line: 2 ch

Formatted: Centered

Formatted: Space After: 0 pt

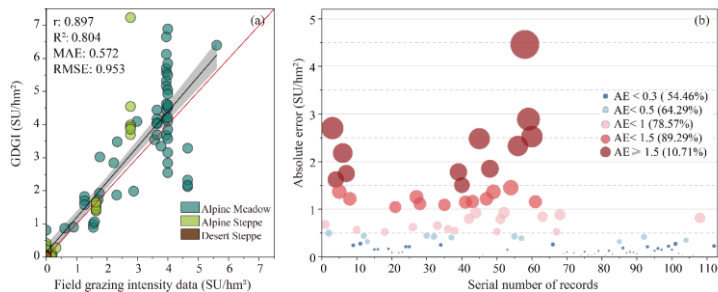
Formatted: Space Before: 0 pt

379
380
381
382
383
384

Figure 5. Uncertainty analysis of grazing intensity maps based on ET and Monte Carlo methods. (a) MRE of grazing intensity maps from 1990 to 2020. (b) spatial distribution of MRE in grazing intensity. (c) spatial distribution of STD in grazing intensity.

3.2.3 Validation of the GDGI dataset

After firstly initially, employing county-level livestock census data as a benchmark for quality control, we obtained the annual Gridded Dataset of Grazing Intensity maps final annual gridded datasets for grazing intensity (GDGI) across the QTP spanning 31 years from 1990 to 2020. We firstly firstly confirmed the accuracy of the GDGI dataset based on 112 field grazing intensity records at 68 sites (see Table S3 in Supplementary file for details), which ranged from 0 to 5.61 sheep unit per hectare (SU/hm²), and covered three main grasslands on the QTP: the alpine steppe (N=62), alpine meadow (N=46), and alpine desert steppe (N=4). The GDGI dataset was assessed by undertaking a comparative accuracy assessment between it and the field grazing intensity data (Figure 5a6a). It can be seen that in general, our dataset was highly consistent with the reference ground-truth validation data, with $R^2 = 0.804$, MAE = 0.572 SU/hm², and RMSE = 0.953 SU/hm². Moreover, the absolute errors between the GDGI data and the field grazing intensity data were relatively small, with more than half of the records having an error below 0.3 SU/hm², 78.57% below 1.0 SU/hm² and 89.29% below 1.5 SU/hm² (Figure 5b6b).

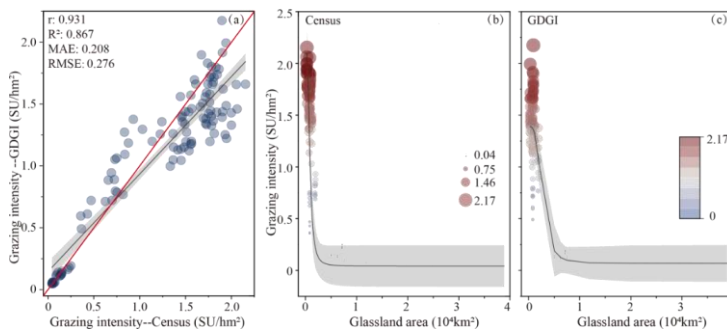


Formatted: Centered

399

400 Figure 56. Validation of the GDGI dataset using 112 field grazing intensity records at the pixel scale: (a) linear
401 fitting results; (b) absolute error (AE) distribution. (Field data see Table S3 in Supplementary file for details).

402 We further validated the precision of the GDGI dataset using the township-level livestock census
403 data. Encouragingly, the evaluation results showed that the GDGI dataset has excellent performance at
404 the township scale (Figure 6a7a), with R^2 of 0.867, MAE of 0.208 SU/hm^2 , and RMSE of 0.276
405 SU/hm^2 . In addition, similarly to the census data, the GDGI dataset indicated that some townships with
406 few grasslands are still under high grazing pressure (Figure 6b-7b and -67c).



407

408 Figure 67. Validation of the GDGI dataset using census livestock data at the township level: (a) linear fit of
409 predicted number and census data; (b-c) logistic fit of grazing intensity data and grassland area.

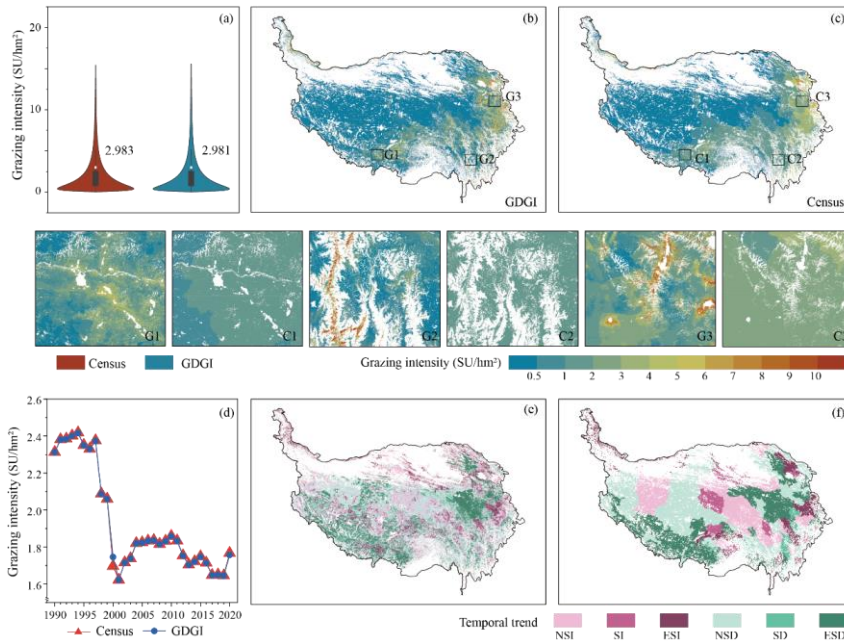
Formatted: Space Before: 0 pt

410 3.3.4 Spatio-temporal variations of grazing intensity

Formatted: Space After: 6 pt

411 In terms of the temporal trends of grazing intensity, the GDGI dataset overall exhibited consistent
412 trends with the livestock census data (Figure 7d8d-7d8f). Specifically, the census data indicated the
413 livestock numbers remained high and largely stable from 1990 to 1997, followed by a sharp decline
414 from 1997 to 2001, and then remained a period of fluctuation post-2001, which was successfully
415 captured by the GDGI dataset. Moreover, the spatial heterogeneity of grazing intensity within the
416 counties over the QTP was also effectively reflected by the GDGI dataset, a characteristic not
417 illustrated by the census dataset. For example, areas of high grazing intensity were concentrated in the
418 northeastern and south-central regions of the plateau, mainly including the eastern part of Qinghai
419 Province, the southwestern part of Gansu Province, the northwestern part of Sichuan Province, and the
420 eastern region of the Tibet Autonomous Region (Figure 7e-8e and 7f8f).

421 Over the past 31 years, 63.95% of the plateau's grassland showed a decreasing trend in grazing
 422 intensity, with 49.80% showing significant decreases, primarily located in the eastern Sanjiangyuan
 423 area and the southwestern region of the QTP (Figure 7e-8c and 7f8f). Meanwhile, grazing intensity was
 424 increasing in 36.05% of the grassland, but most of them (60.16%) did not reach the level of
 425 significance and were mainly distributed in the northeastern plateau (Figure 7e-8c and 7f8f).



426
 427 Figure 78. Validation of the GDGI maps using the census grazing data from 1990 to 2020: (a) violin plot of the
 428 census data and the predicted value; (b-c) spatial distribution in SU per pixel; (d) temporal change in SU per year
 429 (only including 124 counties with livestock census data); (e-f) spatial distribution of SU changes tested by sen's
 430 slope and Mann-Kendall. Note: ESI for Extremely Significant Increase (slope>0 & p<0.01); SI for Significant
 431 Increase (slope>0 & p<0.05); NSI for Non-significant increase (slope>0 & p>0.05); ESD for Extremely
 432 Significant Decrease (slope<0 & p<0.01); SD for Significant decrease (slope<0 & p<0.05); NSD for
 433 Non-significant decrease (slope<0 & p>0.05).

434 4 Discussion

435 4.1 Comparison with other grazing intensity maps

436 To further assess the effectiveness and reliability of the developed GDGI dataset, the mapping
 437 results were juxtaposed with seven publicly available grazing intensity maps covering the QTP (Table
 438 24). It can be seen that despite their public availability, these maps lacked both in spatial and temporal
 439 resolution when juxtaposed with the GDGI maps. Our analysis was extended to four openly accessible
 440 gridded livestock datasets, including GI-Sun (Sun et al., 2021), ALCC (Liu, 2021), GI-Meng (Meng
 441 et al., 2023) and GLWs (Gilbert et al., 2018). Among the GLW series, GLW3 and GLW4 were chosen
 442 owing to their superior performances over GLW1 and GLW2, as indicated by Gilbert et al. (2018). [△]

Formatted: Space Before: 0 pt

443 commonality among all five maps was the consistency for the spatial patterns of grazing intensity, with
444 prevalent high and low intensities in the northeast and northwest regions, respectively (Figure 9).
445 However, these maps differed significantly in terms of accuracy. As the grazing intensity maps of
446 GLWs and ALCC were produced based on the livestock census data in 2001 and 2015, an accuracy
447 comparison for the corresponding years was conducted among the five datasets both at county and
448 township scale. Observations at the county scale indicate that all four datasets, with the exception of
449 GI-Sun, are largely in alignment with the county census data (Figure 9b). When examined at the
450 township scale, GI-Sun and GLW demonstrate the most significant discrepancies, with MRE
451 surpassing 68%. ALCC and GI-Meng follow, recording MREs of 30.69% and 38.80%, respectively.
452 Additionally, the GDGI shows the highest degree of accuracy in relation to the township census data,
453 as indicated by the lowest MAE and RMSE values (Figure 9c). Moreover, the GDGI dataset spanning
454 31 years (1990-2020) earmarked it as a more suitable choice for long-term studies in comparison to the
455 other four datasets. Regarding spatial distribution, the overall patterns of these grazing maps are largely
456 consistent, exhibiting higher density patterns in the southeast and lower in the northwest. However,
457 notable discrepancies are still apparent in the finer details. In general, in terms of visually representing
458 the spatial distribution of livestock, the GDGI maps exhibit the best performance.

459 ~~A commonality among all five maps was the consistency for the spatial patterns of grazing intensity,~~
460 ~~with prevalent high and low intensities in the northeast and northwest regions, respectively (Figure 89).~~
461 ~~However, these maps differed significantly in terms of accuracy. As the grazing intensity maps of~~
462 ~~GLWs and ALCC were produced based on the livestock census data in 2001 and 2015, an accuracy~~
463 ~~comparison for the corresponding years was conducted among the five datasets based on the livestock~~
464 ~~census data in 2001 and 2015 at county and township scale. At the county scale, the livestock~~
465 ~~distribution characteristics of the four datasets, except for GI Sun, are consistent with the county~~
466 ~~census data (Figure 9b). At the township scale, GI Sun and GLW exhibit the highest errors, with MRE~~
467 ~~exceeding 68%; ALCC and GI Meng respectively show 31% and 39%, while GDGI has the smallest~~
468 ~~error, at only 21%. Furthermore, GDGI exhibited the closest to the census data, as evidenced by the~~
469 ~~fact that MAE and RMSE are lowest (Figure 9c). It was observed from the scatter diagrams that R^2~~
470 ~~between the predicted and livestock statistic data for GI Sun, ALCC, and GLWs are lower than 0.6,~~
471 ~~which is significantly lower than the accuracy of GDGI (R^2 exceeds 0.9) (Figure 8a). Furthermore,~~
472 ~~GDGI exhibited the closest to the census data, as evidenced by the fact that MAE and RMSE are less~~
473 ~~than 1 (Figure 8b, 8c). Moreover, the GDGI dataset spanning 31 years (1990-2020) earmarked it as a~~
474 ~~more suitable choice for long-term studies in comparison to the other four datasets. Regarding spatial~~
475 ~~distribution, the overall patterns of these grazing maps are largely consistent, exhibiting higher density~~
476 ~~patterns in the southeast and lower in the northwest. However, notable discrepancies are still apparent~~
477 ~~in the finer details. In general, in terms of visually representing the spatial distribution of livestock, the~~
478 ~~GDGI maps exhibit the best performance.~~

479 The above advantageous of the GDGI dataset are understandable. First, the livestock census data
480 used in GDGI is more detailed, aiding in enhancing the accuracy of the estimation results. Specifically,
481 GI-sun, ALCC, GI-Meng and GDGI all use county-level livestock statistics to map grazing intensity,
482 whereas GLW3 and GLW4 are based on provincial-level census data to map, which results in their
483 accuracy lagging significantly behind the four other datasets (Nicolas et al., 2016; Sun et al., 2021).
484 Second, grazing densities are estimated by dividing the number of livestock from the statistical data,
485 after a mask excluding theoretical unsuitable grazing areas. However, these maps differ in their
486 definitions of suitable grazing areas. In this study, as with the GI-sun and GI-Meng maps, we

Formatted: Font color: Auto

Formatted: Font color: Red

Formatted: Space Before: 6 pt

Formatted: Space Before: 6 pt

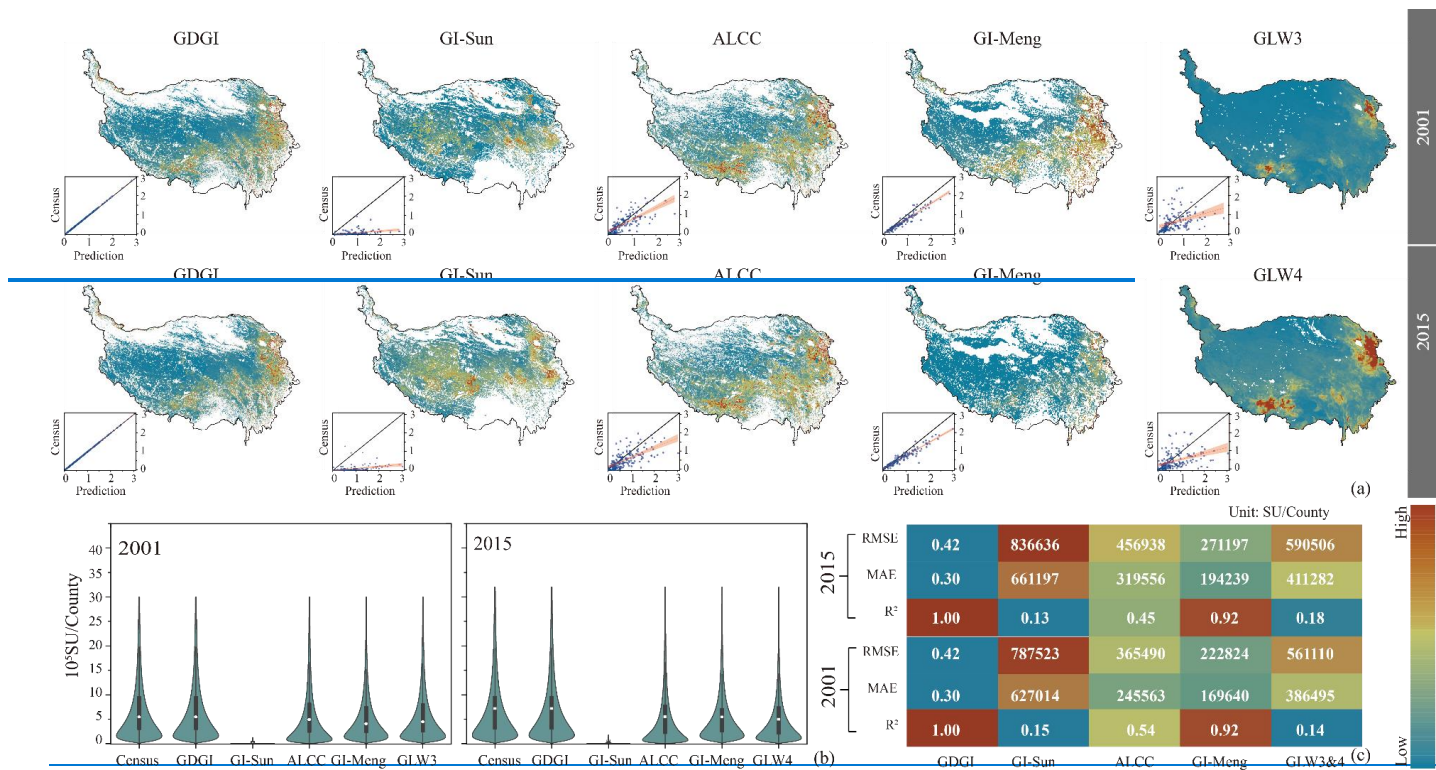
487 considered grazing to occur only on grasslands, and further excluded unsuitable areas such as high
488 elevations and steep slopes. This kind of definition is clearly more reasonable than the GLW series,
489 which removed only water bodies, urban core areas, and protected areas with relatively tight
490 regulations of human activity (Mcsherry and Ritchie, 2013; He et al., 2022). However, the GI-Meng
491 dataset considers the core areas of protected areas as grazing-free region, it does not match the actual
492 situation on the QTP (Jiang et al., 2023; Li et al., 2022b; Zhao et al., 2020). Those different thresholds
493 for the definition of suitable grazing areas are account for the fact each map has different theoretical
494 grazing regions. Third, these maps decompose the livestock census data to pixels based on different
495 mathematical theories, which also leads to differences in prediction accuracy across maps. Specifically,
496 ALCC used a multivariate linear regression algorithm to predict grazing intensity, which has been
497 shown to be significantly inferior to the RF machine learning method employed by GI-Meng, GLW3
498 and GLW4 (Nicolas et al., 2016; Li et al., 2021). In this study, we used the ET model to predict
499 livestock numbers and achieved higher accuracy accordingly. Finally, differences in the selection of
500 factors affecting livestock distribution across maps may also lead to differences in map accuracy.
501 Specifically, GI-sun only used the NPP as indicator, but it is not simply linearly related to grazing
502 intensity (Sun et al., 2021; Ma et al., 2022; Gilbert et al., 2018). ALCC considered the population
503 density, NPP, and terrain as indicators, which are also incomplete considerations of the influencing
504 factors. On the other hand, GLW series dataset considered 12 factors, such as NDVI, EVI, population
505 distribution and elevation. GI-Meng dataset incorporated 14 factors including NDVI, soil PH, available
506 nitrogen, available phosphorus, and available potassium. However, GLWs and GI-Meng ignored the
507 decrease in the prediction accuracy due to redundancy among the factors. In this study, we selected
508 factors related to grazing activities including terrain, climate, environment and social factor, and
509 constructed a prediction model with seven factors including population density, elevation, climate, and
510 HNPP. Unlike other livestock products, this study used HNPP for the first time to replace the
511 commonly used NPP, or NDVI, or EVI as indicator, which has be proved to be more accurately
512 expressed the relationship between livestock and grassland (Huang et al., 2022).

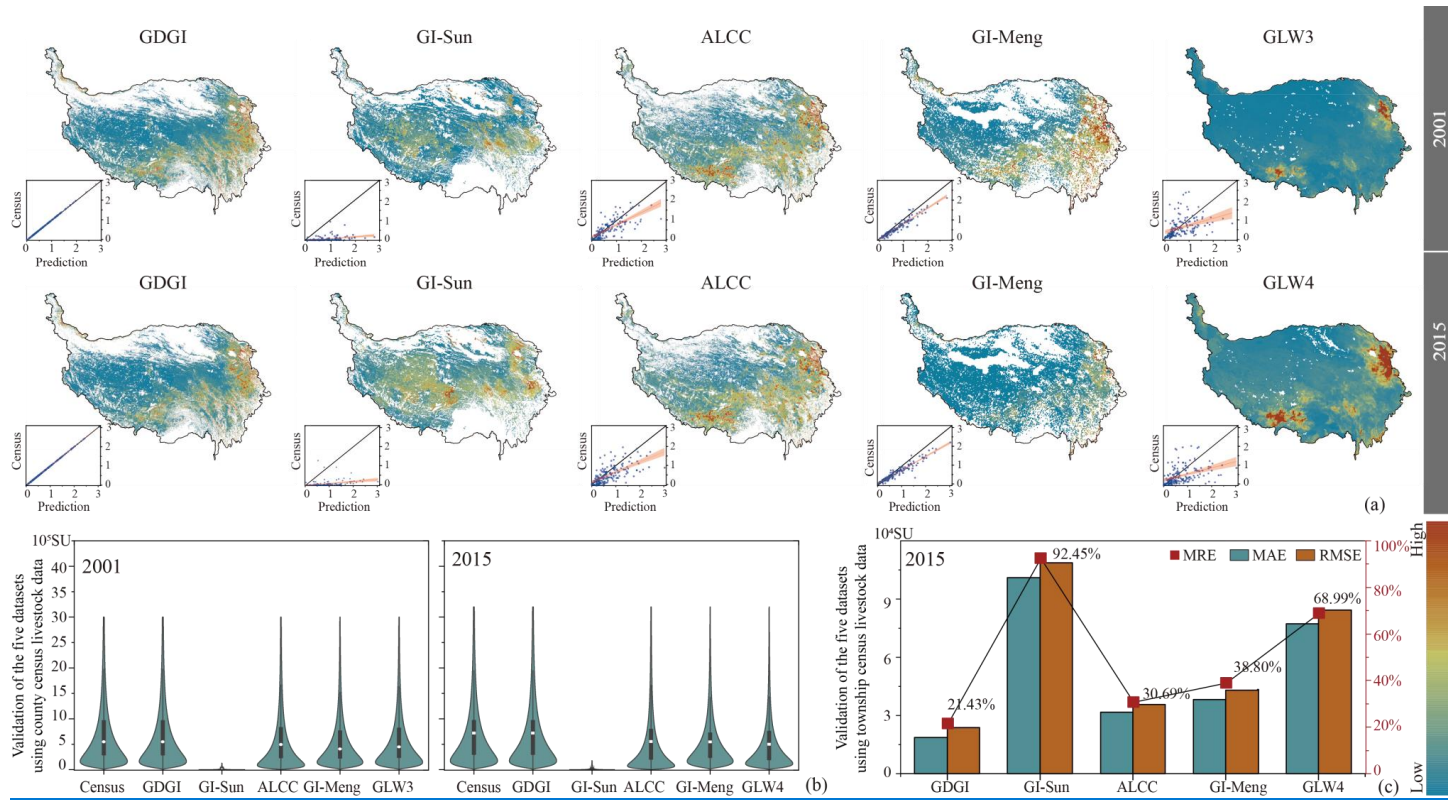
513 Table 24. Summary of map-derived parameters for this study and other seven public gridded livestock datasets covering the QTP.

Dataset	Accessibility	Census	Temporal resolution	Spatial resolution	Period (years)	Method	Livestock type
GDGI	Yes	County	annual	100 m	1990-2020 (31)	ET	Standard SU
GLW3	Yes	Province/sub-Province	annual	0.083° (≈ 10 km)	2001 (1)	RF	Cattle, ducks, pigs, chickens,
GLW4	Yes	Province/sub-Province	annual	0.083° (≈ 10 km)	2015 (1)	RF	sheep, goats
GI-Sun	Yes	County	five-year interval	1 km	1990-2015 (6)	LRA	Standard SU
ALCC	Yes	Province/sub-Province	annual	250 m	2000-2019 (20)	MLR	Standard SU
GI-Meng	Yes	County	annual	0.083° (≈ 10 km)	1982-2015 (34)	RF	Standard SU
GI-Li	No	County	five-year interval	1 km	2000-2015 (4)	DNN	Cattle and sheep
GI-Zhan	No	County	season	15" (≈ 500 m)	2020 (2)	RF	Standard SU

514 Note: LRA is the abbreviation of linear regression analysis.

515





517

518 Figure 89. Comparisons of different grazing datasets for the years 2001 and 2015: (a) spatial patterns; (b) predicted livestock number and census data at county scale; (c) accuracy evaluation
 519 between predicted livestock number and [statistic census data at township scale data](#).

520 4.2 Spatial heterogeneity of grazing intensities

521 In general, the multiyear average grazing intensity on the QTP increased from west to east during
522 1990 to 2020, with broad spatial heterogeneity (Figure 78). Highest grazing intensity was found mainly
523 in the northeastern and south-central regions of the Plateau (mostly higher than 5.0 SU/hm²), while
524 they were lowest in the northwest (mostly less than 1.0 SU/hm²). Over the past 31 years, the average
525 grazing intensity decreased across most of the Plateau, but 36.05% of the entire QTP grassland still
526 encountered continuous grazing intensity increase, especially in the northeastern regions (Figure 78).

527 The spatial heterogeneity of grazing intensities on the QTP may be attributed to the following
528 reasons. First, complex geographic and climatic conditions on the QTP determine the heterogeneity of
529 grassland, which in turn affects livestock distribution (Wang et al., 2018; Wei et al., 2022). In general,
530 the grazing intensity patterns shown in the GDGI maps are basically consistent with the stocking rate
531 threshold patterns in the QTP grasslands, both decreased from east to west (Zhu et al., 2023a). This
532 phenomenon partially reflects the heterogeneity of the grasslands, as the alpine meadows and the
533 steppes mainly distributed in the east and the west, respectively. Second, the dynamics of
534 socio-economic development are obviously another important factors determining grazing intensity. In
535 areas falling behind in terms of the socio-economic indicators, herders prefer to increase livestock in
536 efforts to improve household incomes, leading to greater pressure on grasslands in these regions (Fang
537 and Wu, 2022). In addition, the perceived increases in human population also resulted in the
538 considerably increased need to more livestock (Wei et al., 2022).

539 ~~(Ye et al., 2020)Third, the grazing intensity patterns across the QTP partially reflected the effects of~~
540 ~~management policies launched in different periods. For example, the grazing intensity on the QTP~~
541 ~~grassland increased substantially in the early 1990s, likely due to the launch of the household contract~~
542 ~~responsibility system. Moreover, the grazing intensity decreased in the from late 1990s 1997 and to~~
543 ~~early 2000s 2001 (Figure 7d8d), reflecting the implement of several strict government ecological~~
544 ~~conservation programs, such as Grassland Law of the People's Republic of China" Soil and Water~~
545 ~~Conservation Law of the People's Republic of China the grazing withdrawal program, conversion of~~
546 ~~eroplant to grassland and ecological subsidy and award system. Finally, natural disasters have also~~
547 ~~been an important cause of the drastic reduction in livestock numbers. For example, the snow disasters~~
548 ~~that occurred in Naqu in 1997-1998, central Tibetan Plateau, resulted in the loss of 820,000 livestock~~
549 ~~(Ye et al., 2020). In the early 20th century, in response to areas suffering from overgrazing and~~
550 ~~grassland degradation, China implemented measures such as: the grazing withdrawal program,~~
551 ~~conversion of eroplant to grassland and ecological subsidy and award system. The grazing intensity~~
552 ~~dynamics across the QTP are partly reflective of the impacts of various management policies that have~~
553 ~~been implemented over distinct periods. For example, a significant increase in grazing intensity on the~~
554 ~~QTP was observed in the early 1990s, potentially a direct result of the introduction of the household~~
555 ~~contract responsibility system. Moreover, the grazing intensity experienced a pronounced decline from~~
556 ~~1997 to 2001, as illustrated in Figure 8d, indicative of the adverse effects of natural disasters. Notably,~~
557 ~~the severe snowstorms that struck Naqu in the central QTP during 1997-1998 are documented to have~~
558 ~~caused the mortality of over 820,000 livestock (Ye et al., 2020). Figure 8d further delineates a~~
559 ~~considerable upsurge in grazing intensity on the QTP between 2000 and 2010, aligning with the trends~~
560 ~~reported by Sun et al. (2021) and Li et al. (2021). This observed increase may be attributed to a~~
561 ~~rebound in grazing activity following the aforementioned natural disasters. In addition, Figure 8d~~

562 indicates a sustained decrease in grazing intensity post-2010 across the plateau, which can be
563 predominantly ascribed to the implementation of extensive ecological conservation projects.

Formatted: Font color: Green

565 4.3 Implications for grazing management

566 Nearly half of the grasslands on the QTP have been reported to be degraded over the past four
567 decades (Wang et al., 2018; Dong et al., 2020), with some reports even indicating that the degraded
568 grassland has reached 90% (Wang et al., 2021). It is widely recognized that overgrazing is the
569 predominant and most pervasive unsustainable human activity continuing to drive grassland
570 degradation on the QTP (Wang et al., 2018; Chen et al., 2019). Generally, these degraded grassland
571 on the QTP can be effectively restored by adaptive management (Wang et al., 2022). However, better
572 management of grasslands requires a deeper understanding of the anthropogenic activities, which still
573 remain an important challenge and can be effectively addressed by the GDGI dataset.

574 According to the GDGI maps generated in this study, high-intensity grazing activities are mainly
575 concentrated in the northeastern as well as the south-central part of the QTP, with the grazing intensity
576 in some areas even nearly more than ten times than the average value of the entire plateau (Figure
577 [5b6b](#)), and have exceeded the stocking rate threshold of these grasslands (Zhu et al., 2023a). Population
578 growth and the related increasing livelihood demands is one of the main reasons for this increase. To
579 meet daily needs and enhance household income, the herders have endeavored to increase livestock,
580 thereby intensifying grazing pressures on the grasslands over the QTP (Fang and Wu, 2022; Abu
581 Hammad and Tumeizi, 2012). Although the current average grazing intensity in the northwest QTP
582 (around 1.0 SU/hm²) is below their average stocking rate threshold (around 1.5 SU/hm²) (Zhu et al.,
583 2023a), the grassland management should still be given adequate attention. Because as the most arid
584 areas with low stocking rate threshold on the QTP, the grazing intensity in this region has been
585 increasing in recent years. Nevertheless, it must be noted that the stocking rate threshold may exceed
586 the carrying capacity, because it is predicted to lead to an extreme grassland degradation (Zhu et al.,
587 2023a). The GDGI dataset also showed a similar pattern between the grazing intensity data and the
588 WorldPop data near the built-up areas, indicating higher grazing intensity around settlements than other
589 regions on the QTP. In addition, the GDGI dataset also indicate that from 1990 to 2020, although the
590 grazing intensity of the Plateau has generally decreased, the hotspot areas for grazing activities have
591 remained almost unchanged. This implies that these regions should be the focus of adaptive grassland
592 management to effectively prevent grassland degradation, mainly based on the grass–livestock balance
593 which varies by time and space.

594 Encouragingly, the GDGI dataset show that the grazing intensity for two-thirds of the entire QTP
595 grassland decreased over the past 31 years, which is also consistent with other studies (Sun et al., 2021;
596 Li et al., 2021). Recent decades of biodiversity protection, active restoration projects as well as
597 management measures, such as nature reserves, grazing exclusion, part grazing ban combined with
598 fencing enclosure, are believed to have driven these decrease (Deng et al., 2017; Li and Bennett, 2019).
599 In addition, most grassland in the eastern Sanjiangyuan, the mid-eastern Changtang, and the northern
600 foothills of the Himalayas, showed a significant decrease with grazing intensity (Figure [5e6c](#)),
601 indicating the importance of protected areas on preventing overstock and grassland degradation.
602 Meanwhile, the GDGI maps also show that the grazing density varies greatly among protected areas,

603 possibly owing to the difference in policy implementation. For instance, it can be seen from the GDGI
604 maps that grazing intensity are increasing in some protected areas, especially several wetland nature
605 reserves on the Zoige plateau (Figure 5e6c). Moreover, the average grazing intensity in all nature
606 reserves on the QTP has overall increased from 1990 to 2020, although their increase rate is much
607 lower than the non-protected areas ($0.0125 \text{ SU/hm}^2 \cdot 10a$ vs $0.0304 \text{ SU/hm}^2 \cdot 10a$), which implies that
608 grassland management in protected areas still needs to be strengthened on the QTP.

609 The grazing initiatives in alignment with the Sustainable Development Goals (SDGs) on the QTP
610 can benefit from the GDGI dataset. Firstly, determination a reasonable stocking rate is vital to prevent
611 overstocking of the pastures, which will possibly induce extreme grassland degradation (Zhu et al.,
612 2023a). Stocking rate determination can be optimized by using our grazing intensity maps and the
613 stocking rate threshold maps of the QTP. Secondly, the GDGI maps can contribute to strategic
614 placement of fence, which is a common practice adopted to prevent grassland degradation on the QTP.
615 Building fences in areas with high grazing intensity and exceeding the carrying capacity can improve
616 the effectiveness of fence construction (Zhou et al., 2023; Zhang et al., 2023). Thirdly, the GDGI
617 dataset can provide a solid support for promoting effective nature reserve management, which in total
618 covering nearly one third of the entire QTP. For example, the GDGI maps showed that grazing
619 activities still exist in most nature reserves on the Plateau, although most of them have significantly
620 lower grazing intensities compared with their adjacent non-protected areas. By using the GDGI maps,
621 the conflict between ecological protection and grazing activities in nature reserves can be alleviated.
622 Finally, our grazing intensity maps can act as a basic dataset to support other grassland-related policies.
623 Currently, these policies on the QTP often adopt a one-size-fits-all approach to determine the carrying
624 capacity and carry out ecological compensation, which may lead to overstock or unfair financial
625 distribution (Wang et al., 2022). The grassland management strategies balancing carrying capacity and
626 stocking rates are more likely to result in optimal management choices for policymakers and
627 stakeholders, and our GDGI maps can contribute to this decision-making processes.

628 4.4 Uncertainties and limitations

629 Although this study has collected as reliable datasets as possible, users of the GDGI products
630 should be cognizant of inherent uncertainties and limitations within these datasets. Notably, the mean
631 relative error of the GDGI dataset spanning 1990 to 2020 was recorded at 4.2% (Figure 4a), calculated
632 from the average errors across 182 counties within the QTP that had accessible livestock census data.
633 Furthermore, approximately 8.26% of grassland areas exhibited a relative error exceeding 1.0 SU/hm^2
634 (Figure 4b). Such discrepancies arise from several limitations that were subsequently propagated to the
635 final grazing intensity maps, thereby contributing to the dataset's overall uncertainties.

636 Firstly, the estimations of grazing intensities were fundamentally conservative, primarily due to the
637 lack of comprehensive input data. Livestock numbers, derived from year-end data at the county level,
638 inadvertently led to underestimations of grazing intensity by not accounting for livestock off-take rates.
639 Likewise, the evaluation focused solely on livestock grazing intensity, excluding wild herbivores and
640 forage-dependent livestock, which potentially underestimate actual grazing pressures on the QTP.
641 Additionally, despite identifying seven main factors influencing livestock distribution, the study did not
642 encompass all potential factors, such as fencing, forage availability, road proximity, and season
643 transformation in grazing practices. Moreover, to align with county-scale livestock census data, we
644 averaged the environmental factors at the county-scale. Although this approach have been widely used

645 on the hypothesis that a consistent causal relationship between livestock intensity and environmental
646 factors persists across various scales (Robinson et al., 2014; Nicolas et al., 2016; Li et al., 2021; Meng
647 et al., 2023) (Robinson et al., 2014; Nicolas et al., 2016; Li et al., 2021; Meng et al., 2023), it might
648 oversimplify the intricate dynamics between grazing intensity and lead to a certain degree of estimation
649 inaccuracies. In addition, the reliance on linear extrapolation to Supplementary missing gridded 100-m
650 population density data from 1990-1999 introduced further uncertainties due to the limited resolution
651 (1-km) and interval (5-year) of the ChinaPop dataset.

652 Secondly, the modeling process for mapping grazing intensity also suffered from several challenges.
653 For instance, the ET model was trained with a limited sample size of 4,998 and applied to a vast area
654 consisting of 150 million pixels, which could compromise the model's accuracy. In addition, despite the
655 ET model's design to reduce overfitting risks by using randomly selected features and partition decision,
656 the potential for overfit effects still remained, particularly when faced with a high number of output
657 classes or insufficient sample sizes (Geurts et al., 2006; Galelli and Castelletti, 2013) (Geurts et al.,
658 2006; Galelli and Castelletti, 2013). In fact, this limitation was evident in this study, as the
659 generalization capability of the ET model was restricted by the disparity between the number of
660 training samples and the total number of pixels, leading to predictions that often exceeded actual
661 livestock census (Figure 4a).

662 Thirdly, our methodological framework for high-resolution gridded grazing dataset mapping was
663 developed based on the assumption that all grassland were accessible to livestock. However, in reality,
664 the amount of available grassland was less due to fencing and grazing bans on the QTP (Zhan et al.,
665 2023). Moreover, transhumant herders generally follow a seasonal calendar for summer pastures and
666 winter pastures on the QTP. However, we did not consider this seasonal movements due to data
667 limitations, which further restrict the analysis of seasonal livestock distribution patterns (Kolluru et al.,
668 2023). Additionally, the model's reliance on human population as a proxy for livestock locations
669 overlooked the possibility of high grazing intensity in areas with low human populations on the QTP,
670 particularly in regions designated for summer pastures.

671 Finally, it is important to note that gathering livestock census data in the Qinghai-Tibet Plateau
672 presents significant challenges, leading to a scarcity of livestock validation data in this study,
673 particularly at the township and pixel scales. This limitation may, to some extent, impact the reliability
674 of the grazing intensity data we have presented.
675

676 In summary, all these limitations associated with input data, the modeling process, and the
677 methodological framework collectively contribute to the uncertainties and potentially reduce accuracy
678 of the GDGI maps. We henceforth recommend that future research should aim to incorporate more
679 detailed data, consider additional influential factors, enhance key dataset's time-series consistency, and
680 refine the methodological framework to improve the accuracy of grazing intensity mapping.

683 5 Data availability

684 The annual gridded grazing intensity maps of the QTP spanning from 1990 to 2020 are accessible
685 at the following link:
686 <https://doi.org/10.5281/zenodo.13141090><https://doi.org/10.5281/zenodo.10851119> (Zhou et al., 2024).
687 Each map is catalogued by year and recorded in GeoTIFF format, with values represented in SU/hm²

Formatted: Font color: Auto

Formatted: Font color: Green

688 per year. These datasets, with a spatial resolution of 100 m and annual temporal resolution, utilize the
689 WGS-1984-Albers geographic coordinate system. To streamline data transfer and download processes,
690 the comprehensive 31-year dataset has been compressed into a ZIP file, readily available for download
691 and compatible with Geographic Information System (GIS) software for viewing.

692 **6 Conclusions**

693 In this study, we introduce a framework utilizing ET machine learning algorithms to achieve
694 fine-scale livestock spatialization, subsequently generating the GDGI dataset across the QTP. The
695 GDGI has a spatial resolution of 100 m and expands 31 years from 1990 to 2020. It is consistent with
696 livestock census data of the QTP, and has a relatively higher precision than previous datasets with
697 MAE of 0.006 SU/hm² based on 4,998 independent test samples. In addition, the accuracy evaluations
698 at both pixel-level and township-level underscore the outstanding reliability and applicability of the
699 GDGI dataset, which can successfully capture the spatial heterogeneity and variation in grazing
700 intensities in greater details. Moreover, comparisons between the GDGI dataset and other existing
701 grazing map products further proved the robust and efficient of our dataset, and demonstrate the
702 validity of the proposed framework in the research of livestock spatialization. The GDGI dataset
703 presented in this study can address existing limitations and enhance the understanding of grazing
704 activities on the QTP. This, in turn, can aid in the rational utilization of grasslands and facilitate the
705 implementation of informed and sustainable management practices.

706 **Supplementary.**

707 For gridded datasets influencing grazing that are not directly available, or that do not meet
708 spatio-temporal resolution requirements—such as those pertaining to population density, temperature,
709 precipitation, and HNPP—we have delineated the processing or creation procedures in the
710 [SupplementarySupplementary](#) file.

711 **Author contributions.**

712 T.L. conceived the research; J.Z. and J.N. performed the analyses and wrote the first draft of the
713 paper; N.W. and T.L. reviewed and edited the paper before submission. All authors made substantial
714 contributions to the discussion of content.

715 **Competing interests.**

716 The authors declare that they have no conflict of interest.

717 **Acknowledgements.**

718 We would like to thank the Bureau of Statistics of each county over the QTP for providing the
719 census livestock data.

720 **Financial support.**

721 This research was supported by the Second Tibetan Plateau Scientific Expedition and Research

722 Program (STEP), Ministry of Science and Technology of the People's Republic of China (grant no.
723 2019QZKK0402) and the National Natural Science Foundation of China (grant no. 42071238).

724 References

- 725 [Abu Hammad, A. and Tumeizi, A.: Land degradation: socioeconomic and environmental causes and](#)
726 [consequences in the eastern Mediterranean, *Land. Degrad. Dev.*, 23, 216-226,](#)
727 <https://doi.org/10.1002/ldr.1069>, 2012.
- 728 [Ahmad, M. W., Reynolds, J., and Rezgui, Y.: Predictive modelling for solar thermal energy systems: A](#)
729 [comparison of support vector regression, random forest, extra trees and regression trees, *J. Clean*](#)
730 [Prod., 203, 810-821, <https://doi.org/10.1016/j.jclepro.2018.08.207>, 2018.](#)
- 731 [Alexander, P., Prestele, R., Verburg, P. H., Armeth, A., Baranzelli, C., Batista e Silva, F., Brown, C.,](#)
732 [Butler, A., Calvin, K., and Dendoncker, N.: Assessing uncertainties in land cover projections, *Glob.*](#)
733 [Chang. Biol., 23, 767-781, 2017.](#)
- 734 [Allred, B. W., Fuhlendorf, S. D., Hovick, T. J., Dwayne Elmore, R., Engle, D. M., and Joern, A.:](#)
735 [Conservation implications of native and introduced ungulates in a changing climate, *Glob. Chang.*](#)
736 [Biol., 19, 1875-1883, <https://doi.org/10.1111/gcb.12183>, 2013.](#)
- 737 [Breiman, L.: Random Forests, *Mach. Learn.*, 45, 5-32, <https://doi.org/10.1023/A:1010933404324>,](#)
738 2001.
- 739 [Cai, Y. J., Wang, X. D., Tian, L. L., Zhao, H., Lu, X. Y., and Yan, Y.: The impact of excretal returns](#)
740 [from yak and Tibetan sheep dung on nitrous oxide emissions in an alpine steppe on the](#)
741 [Qinghai-Tibetan Plateau, *Soil. Biol. Biochem.*, 76, 90-99,](#)
742 <https://doi.org/10.1016/j.soilbio.2014.05.008>, 2014.
- 743 [Chang, J. F., Ciais, P., Gasser, T., Smith, P., Herrero, M., Havlik, P., Obersteiner, M., Guenet, B., Goll,](#)
744 [D. S., Li, W., Naipal, V., Peng, S. S., Qiu, C. J., Tian, H. Q., Viovy, N., Yue, C., and Zhu, D.: Climate](#)
745 [warming from managed grasslands cancels the cooling effect of carbon sinks in sparsely grazed and](#)
746 [natural grasslands, *Nat. Commun.*, 12, 118, <https://doi.org/10.1038/s41467-020-20406-7>, 2021.](#)
- 747 [Chen, Y. Z., Ju, W. M., Mu, S. J., Fei, X. R., Cheng, Y., Propastin, P., Zhou, W., Liao, C. J., Chen, L. X.,](#)
748 [Tang, R. J., Qi, J. G., Li, J. L., and Ruan, H. H.: Explicit Representation of Grazing Activity in a](#)
749 [Diagnostic Terrestrial Model: A Data - Process Combined Scheme, *J. Adv. Model. Earth. Sy.*, 11,](#)
750 [957-978, <https://doi.org/10.1029/2018ms001352>, 2019.](#)
- 751 [Cortes, C. and Vapnik, V.: Support-vector networks, *Mach. Learn.*, 20, 273-297,](#)
752 <https://doi.org/10.1007/BF00994018>, 1995.
- 753 [Cover, T. and Hart, P.: Nearest neighbor pattern classification, *Ieee. T. Inform. Theory.*, 13, 21-27,](#)
754 <https://doi.org/10.1109/TIT.1967.1053964>, 1967.
- 755 [Dara, A., Baumann, M., Freitag, M., Hölzel, N., Hostert, P., Kamp, J., Müller, D., Prishchepov, A. V.,](#)
756 [and Kuemmerle, T.: Annual Landsat time series reveal post-Soviet changes in grazing pressure,](#)
757 [Remote. Sens. Environ., 239, 111667, <https://doi.org/10.1016/j.rse.2020.111667>, 2020.](#)
- 758 [Deng, L., Zhou, S. G., Wu, P., Gao, L., and Chang, X.: Effects of grazing exclusion on carbon](#)
759 [sequestration in China's grassland, *Earth-Sci. Rev.*, 173, 84-95,](#)
760 <https://doi.org/10.1016/j.earscirev.2017.08.008>, 2017.
- 761 [Dong, S. K., Shang, Z. H., Gao, J. X., and Boone, R. B.: Enhancing sustainability of grassland](#)
762 [ecosystems through ecological restoration and grazing management in an era of climate change on](#)
763 [Qinghai-Tibetan Plateau, *Agr. Ecosyst. Environ.*, 287, 106684,](#)

Formatted: Font: (Default) Times New Roman

Formatted: Indent: Left: 0", Hanging: 1 ch, First line: -1 ch

Formatted: Font: (Default) Times New Roman

Formatted: Font: (Default) Times New Roman

Formatted: Font: (Default) Times New Roman

Formatted: Font: (Default) Times New Roman

Formatted: Font: (Default) Times New Roman

Formatted: Font: (Default) Times New Roman

Formatted: Font: (Default) Times New Roman

Formatted: Font: (Default) Times New Roman

Formatted: Font: (Default) Times New Roman

Formatted: Font: (Default) Times New Roman

Formatted: Font: (Default) Times New Roman

Formatted: Font: (Default) Times New Roman

Formatted: Font: (Default) Times New Roman

Formatted: Font: (Default) Times New Roman

Formatted: Font: (Default) Times New Roman

Formatted: Font: (Default) Times New Roman

Formatted: Font: (Default) Times New Roman

Formatted: Font: (Default) Times New Roman

Formatted: Font: (Default) Times New Roman

Formatted: Font: (Default) Times New Roman

Formatted: Font: (Default) Times New Roman

Formatted: Font: (Default) Times New Roman

764 <https://doi.org/10.1016/j.agee.2019.106684>, 2020.

765 Fang, X. N. and Wu, J. G.: Causes of overgrazing in Inner Mongolian grasslands: Searching for deep
766 leverage points of intervention, *Ecol. Soc.*, 27, <https://doi.org/10.5751/es-12878-270108>, 2022.

767 Feng, R. Z., Long, R. J., Shang, Z. H., Ma, Y. S., Dong, S. K., and Wang, Y. L.: Establishment of
768 *Elymus natans* improves soil quality of a heavily degraded alpine meadow in Qinghai-Tibetan
769 Plateau, China, *Plant. Soil.*, 327, 403-411, <https://doi.org/10.1007/s11104-009-0065-3>, 2009.

770 Fetzel, T., Havlik, P., Herrero, M., Kaplan, J. O., Kastner, T., Kroisleitner, C., Rolinski, S., Searchinger,
771 T., Van Bodegom, P. M., Wirseniuss, S., and Erb, K. H.: Quantification of uncertainties in global
772 grazing systems assessment, *Global. Biogeochem. Cy.*, 31, 1089-1102,
773 <https://doi.org/10.1002/2016gb005601>, 2017.

774 Friedman, J. H.: Greedy function approximation: a gradient boosting machine, *Ann. Stat.*, 29,
775 1189-1232, <https://doi.org/10.1214/aos/1013203451>, 2001.

776 Galelli, S. and Castelletti, A.: Assessing the predictive capability of randomized tree-based ensembles
777 in streamflow modelling, *Hydrol. Earth. Syst. Sc.*, 17, 2669-2684,
778 <https://doi.org/10.5194/hess-17-2669-2013>, 2013.

779 García, R., Aguilar, J., Toro, M., Pinto, A., and Rodríguez, P.: A systematic literature review on the use
780 of machine learning in precision livestock farming, *Comput. Electron. Agr.*, 179, 105826,
781 <https://doi.org/10.1016/j.compag.2020.105826>, 2020.

782 García Ruiz, J. M., Tomás Faci, G., Diarte Blasco, P., Montes, L., Domingo, R., Sebastián, M., Lasanta,
783 T., González Sampérez, P., López Moreno, J. I., Arnáez, J., and Beguería, S.: Transhumance and
784 long-term deforestation in the subalpine belt of the central Spanish Pyrenees: An interdisciplinary
785 approach, *Catena.*, 195, 104744, <https://doi.org/10.1016/j.catena.2020.104744>, 2020.

786 Garrett, R. D., Koh, I., Lambin, E. F., le Polain de Waroux, Y., Kastens, J. H., and Brown, J. C.:
787 Intensification in agriculture-forest frontiers: Land use responses to development and conservation
788 policies in Brazil, *Global. Environ. Chang.*, 53, 233-243,
789 <https://doi.org/10.1016/j.gloenvcha.2018.09.011>, 2018.

790 Geurts, P., Ernst, D., and Wehenkel, L.: Extremely randomized trees, *Mach. Learn.*, 63, 3-42,
791 <https://doi.org/10.1007/s10994-006-6226-1>, 2006.

792 Gilbert, M., Nicolas, G., Cinardi, G., Van Boeckel, T. P., Vanwambeke, S. O., Wint, G. R. W., and
793 Robinson, T. P.: Global distribution data for cattle, buffaloes, horses, sheep, goats, pigs, chickens and
794 ducks in 2010, *Sci. Data.*, 5, 180227, <https://doi.org/10.1038/sdata.2018.227>, 2018.

795 Godfray, H. C. J., Aveyard, P., Garnett, T., Hall, J. W., Key, T. J., Lorimer, J., Pierrehumbert, R. T.,
796 Scarborough, P., Springmann, M., and Jebb, S. A.: Meat consumption, health, and the environment,
797 *Science.*, 361, 243, <https://doi.org/10.1126/science.aam5324>, 2018.

798 Guo, Z. L., Li, Z., and Cui, G. F.: Effectiveness of national nature reserve network in representing
799 natural vegetation in mainland China, *Biodivers. Conserv.*, 24, 2735-2750,
800 <https://doi.org/10.1007/s10531-015-0959-8>, 2015.

801 Han, Y. H., Dong, S. K., Zhao, Z. Z., Sha, W., Li, S., Shen, H., Xiao, J. N., Zhang, J., Wu, X. Y., Jiang,
802 X. M., Zhao, J. B., Liu, S. L., Dong, Q. M., Zhou, H. K., and Yeomans, J. C.: Response of soil
803 nutrients and stoichiometry to elevated nitrogen deposition in alpine grassland on the
804 Qinghai-Tibetan Plateau, *Geoderma.*, 343, 263-268, <https://doi.org/10.1016/j.geoderma.2018.12.050>,
805 2019.

806 He, M., Pan, Y. H., Zhou, G. Y., Barry, K. E., Fu, Y. L., and Zhou, X. H.: Grazing and global change
807 factors differentially affect biodiversity - ecosystem functioning relationships in grassland

Formatted: Font: (Default) Times New Roman

Formatted: Font: (Default) Times New Roman

Formatted: Font: (Default) Times New Roman

Formatted: Font: (Default) Times New Roman

Formatted: Font: (Default) Times New Roman

Formatted: Font: (Default) Times New Roman

Formatted: Font: (Default) Times New Roman

Formatted: Font: (Default) Times New Roman

Formatted: Font: (Default) Times New Roman

Formatted: Font: (Default) Times New Roman

Formatted: Font: (Default) Times New Roman

Formatted: Font: (Default) Times New Roman

Formatted: Font: (Default) Times New Roman

Formatted: Font: (Default) Times New Roman

Formatted: Font: (Default) Times New Roman

Formatted: Font: (Default) Times New Roman

Formatted: Font: (Default) Times New Roman

Formatted: Font: (Default) Times New Roman

Formatted: Font: (Default) Times New Roman

Formatted: Font: (Default) Times New Roman

Formatted: Font: (Default) Times New Roman

Formatted: Font: (Default) Times New Roman

Formatted: Font: (Default) Times New Roman

Formatted: Font: (Default) Times New Roman

Formatted: Font: (Default) Times New Roman

Formatted: Font: (Default) Times New Roman

Formatted: Font: (Default) Times New Roman

Formatted: Font: (Default) Times New Roman

808 ecosystems, *Glob. Chang. Biol.*, 28, 5492-5504, <https://doi.org/10.1111/gcb.16305>, 2022.

809 Heddam, S., Ptak, M., and Zhu, S. L.: Modelling of daily lake surface water temperature from air
810 temperature: Extremely randomized trees (ERT) versus Air2Water, MARS, M5Tree, RF and
811 MLPNN, *J. Hydrol.*, 588, 125130, <https://doi.org/10.1016/j.jhydrol.2020.125130>, 2020.

812 Hu, Y., Cheng, H., and Tao, S.: Environmental and human health challenges of industrial livestock and
813 poultry farming in China and their mitigation, *Environ. Int.*, 107, 111-130,
814 <https://doi.org/10.1016/j.envint.2017.07.003>, 2017.

815 Huang, X. T., Yang, Y. S., Chen, C. B., Zhao, H. F., Yao, B. Q., Ma, Z., Ma, L., and Zhou, H. K.:
816 Quantifying and Mapping Human Appropriation of Net Primary Productivity in Qinghai Grasslands
817 in China, *Agriculture.*, 12, 483, <https://doi.org/10.3390/agriculture12040483>, 2022.

818 Humpenöder, F., Bodirsky, B. L., Weindl, I., Lotze Campen, H., Linder, T., and Popp, A.: Projected
819 environmental benefits of replacing beef with microbial protein, *Nature.*, 605, 90-96,
820 <https://doi.org/10.1038/s41586-022-04629-w>, 2022.

821 Jiang, M. J., Zhao, X. F., Wang, R., Yin, L., and Zhang, B. L.: Assessment of Conservation
822 Effectiveness of the Qinghai-Tibet Plateau Nature Reserves from a Human Footprint Perspective
823 with Global Lessons, *Land.*, 12, 869, <https://doi.org/10.3390/land12040869>, 2023.

824 Kolluru, V., John, R., Saraf, S., Chen, J. Q., Hankerson, B., Robinson, S., Kussainova, M., and Jain, K.:
825 Gridded livestock density database and spatial trends for Kazakhstan, *Sci. Data.*, 10, 839,
826 <https://doi.org/10.1038/s41597-023-02736-5>, 2023.

827 Kumar, P., Abubakar, A. A., Verma, A. K., Umaraw, P., Adewale Ahmed, M., Mehta, N., Nizam Hayat,
828 M., Kaka, U., and Sazili, A. Q.: New insights in improving sustainability in meat production:
829 opportunities and challenges, *Crit. Rev. Food. Sci.*, 1-29,
830 <https://doi.org/10.1080/10408398.2022.2096562>, 2022.

831 Li, M. Q., Liu, S. L., Wang, F. F., Liu, H., Liu, Y. X., and Wang, Q. B.: Cost-benefit analysis of
832 ecological restoration based on land use scenario simulation and ecosystem service on the
833 Qinghai-Tibet Plateau, *Glob. Ecol. Conserv.*, 34, e02006,
834 <https://doi.org/10.1016/j.gecco.2022.e02006>, 2022a.

835 Li, P. and Bennett, J.: Understanding herders' stocking rate decisions in response to policy initiatives,
836 *Sci. Total. Environ.*, 672, 141-149, <https://doi.org/10.1016/j.scitotenv.2019.03.407>, 2019.

837 Li, Q., Zhang, C. L., Shen, Y. P., Jia, W. R., and Li, J.: Quantitative assessment of the relative roles of
838 climate change and human activities in desertification processes on the Qinghai-Tibet Plateau based
839 on net primary productivity, *Catena.*, 147, 789-796, <https://doi.org/10.1016/j.catena.2016.09.005>,
840 2016.

841 Li, S., Wu, J., Gong, J., and Li, S.: Human footprint in Tibet: Assessing the spatial layout and
842 effectiveness of nature reserves, *Sci Total Environ*, 621, 18-29,
843 <https://doi.org/10.1016/j.scitotenv.2017.11.216>, 2018.

844 Li, T., Cai, S. H., Singh, R. K., Cui, L. Z., Fava, F., Tang, L., Xu, Z. H., Li, C. J., Cui, X. Y., Du, J. Q.,
845 Hao, Y. B., Liu, Y. X., and Wang, Y. F.: Livelihood resilience in pastoral communities:
846 Methodological and field insights from Qinghai-Tibetan Plateau, *Sci. Total. Environ.*, 838, 155960,
847 <https://doi.org/10.1016/j.scitotenv.2022.155960>, 2022b.

848 Li, X. H., Hou, J. L., and Huang, C. L.: High-Resolution Gridded Livestock Projection for Western
849 China Based on Machine Learning, *Remote. Sens.*, 13, 5038, <https://doi.org/10.3390/rs13245038>,
850 2021.

851 Lin, G. C., Lin, A. J., and Gu, D. L.: Using support vector regression and K-nearest neighbors for

Formatted: Font: (Default) Times New Roman

Formatted: Font: (Default) Times New Roman

Formatted: Font: (Default) Times New Roman

Formatted: Font: (Default) Times New Roman

Formatted: Font: (Default) Times New Roman

Formatted: Font: (Default) Times New Roman

Formatted: Font: (Default) Times New Roman

Formatted: Font: (Default) Times New Roman

Formatted: Font: (Default) Times New Roman

Formatted: Font: (Default) Times New Roman

Formatted: Font: (Default) Times New Roman

Formatted: Font: (Default) Times New Roman

Formatted: Font: (Default) Times New Roman

Formatted: Font: (Default) Times New Roman

Formatted: Font: (Default) Times New Roman

Formatted: Font: (Default) Times New Roman

Formatted: Font: (Default) Times New Roman

Formatted: Font: (Default) Times New Roman

Formatted: Font: (Default) Times New Roman

Formatted: Font: (Default) Times New Roman

Formatted: Font: (Default) Times New Roman

Formatted: Font: (Default) Times New Roman

Formatted: Font: (Default) Times New Roman

Formatted: Font: (Default) Times New Roman

Formatted: Font: (Default) Times New Roman

Formatted: Font: (Default) Times New Roman

Formatted: Font: (Default) Times New Roman

Formatted: Font: (Default) Times New Roman

852 short-term traffic flow prediction based on maximal information coefficient, *Inform. Sciences.*, 608,
853 517-531, <https://doi.org/10.1016/j.ins.2022.06.090>, 2022.

854 Long, S. J., Wei, X. L., Zhang, F., Zhang, R. H., Xu, J., Wu, K., Li, Q. Q., and Li, W. W.: Estimating
855 daily ground-level NO₂ concentrations over China based on TROPOMI observations and machine
856 learning approach, *Atmos. Environ.*, 289, 119310, <https://doi.org/10.1016/j.atmosenv.2022.119310>,
857 2022.

858 Luo, J. F., Hoogendoorn, C., van der Weerden, T., Saggarr, S., de Klein, C., Giltrap, D., Rollo, M., and
859 Rys, G.: Nitrous oxide emissions from grazed hill land in New Zealand, *Agr. Ecosyst. Environ.*, 181,
860 58-68, <https://doi.org/10.1016/j.agee.2013.09.020>, 2013.

861 Ma, C., Xie, Y., Duan, H., Wang, X., Bie, Q., Guo, Z., He, L., and Qin, W.: Spatial quantification
862 method of grassland utilization intensity on the Qinghai-Tibetan Plateau: A case study on the Selinco
863 basin, *J. Environ. Manage.*, 302, 114073, <https://doi.org/10.1016/j.jenvman.2021.114073>, 2022.

864 Mack, G., Walter, T., and Flury, C.: Seasonal alpine grazing trends in Switzerland: Economic
865 importance and impact on biotic communities, *Environ. Sci. Policy.*, 32, 48-57,
866 <https://doi.org/10.1016/j.envsci.2013.01.019>, 2013.

867 Martinuzzi, S., Radeloff, V. C., Pastur, G. M., Rosas, Y. M., Lizarraga, L., Politi, N., Rivera, L., Herrera,
868 A. H., Silveira, E. M. O., Olah, A., and Pidgeon, A. M.: Informing forest conservation planning with
869 detailed human footprint data for Argentina, *Glob. Ecol. Conserv.*, 31, e01787,
870 <https://doi.org/10.1016/j.gecco.2021.e01787>, 2021.

871 McMillan, H. K., Westerberg, I. K., and Krueger, T.: Hydrological data uncertainty and its implications,
872 *Wiley Interdisciplinary Reviews: Water*, 5, e1319, 2018.

873 McSherry, M. E. and Ritchie, M. E.: Effects of grazing on grassland soil carbon: a global review, *Glob.*
874 *Chang. Biol.*, 19, 1347-1357, <https://doi.org/10.1111/gcb.12144>, 2013.

875 Meng, N., Wang, L. J., Qi, W. C., Dai, X. H., Li, Z. Z., Yang, Y. Z., Li, R. N., Ma, J. F., and Zheng, H.:
876 A high-resolution gridded grazing dataset of grassland ecosystem on the Qinghai-Tibet Plateau in
877 1982-2015, *Sci. Data.*, 10, 68, <https://doi.org/10.1038/s41597-023-01970-1>, 2023.

878 Miao, L. J., Sun, Z. L., Ren, Y. J., Schierhorn, F., and Müller, D.: Grassland greening on the Mongolian
879 Plateau despite higher grazing intensity, *Land. Degrad. Dev.*, 32, 792-802,
880 <https://doi.org/10.1002/ldr.3767>, 2020.

881 Minoofar, A., Gholami, A., Eslami, S., Hajizadeh, A., Gholami, A., Zandi, M., Ameri, M., and Kazem,
882 H. A.: Renewable energy system opportunities: A sustainable solution toward cleaner production and
883 reducing carbon footprint of large-scale dairy farms, *Energ. Convers. Manage.*, 293, 117554,
884 <https://doi.org/10.1016/j.enconman.2023.117554>, 2023.

885 Mulligan, M., van Soesbergen, A., Hole, D. G., Brooks, T. M., Burke, S., and Hutton, J.: Mapping
886 nature's contribution to SDG 6 and implications for other SDGs at policy relevant scales, *Remote.*
887 *Sens. Environ.*, 239, 111671, <https://doi.org/10.1016/j.rse.2020.111671>, 2020.

888 Muloi, D. M., Wee, B. A., McClean, D. M. H., Ward, M. J., Pankhurst, L., Phan, H., Ivens, A. C.,
889 Kivali, V., Kiyong'a, A., Ndinda, C., Gitahi, N., Ouko, T., Hassell, J. M., Imboma, T., Akoko, J.,
890 Murungi, M. K., Njoroge, S. M., Muinde, P., Nakamura, Y., Alumasa, L., Furmaga, E., Kaitho, T.,
891 Öhgren, E. M., Amanya, F., Ogendo, A., Wilson, D. J., Bettridge, J. M., Kiiru, J., Kyobutungi, C.,
892 Tacoli, C., Kang'ethe, E. K., Davila, J. D., Kariuki, S., Robinson, T. P., Rushton, J., Woolhouse, M. E.
893 J., and Fèvre, E. M.: Population genomics of *Escherichia coli* in livestock-keeping households across
894 a rapidly developing urban landscape, *Nat. Microbiol.*, 7, 581-589,
895 <https://doi.org/10.1038/s41564-022-01079-y>, 2022.

Formatted: Font: (Default) Times New Roman

Formatted: Font: (Default) Times New Roman

Formatted: Font: (Default) Times New Roman

Formatted: Font: (Default) Times New Roman

Formatted: Font: (Default) Times New Roman

Formatted: Font: (Default) Times New Roman

Formatted: Font: (Default) Times New Roman

Formatted: Font: (Default) Times New Roman

Formatted: Font: (Default) Times New Roman

Formatted: Font: (Default) Times New Roman

Formatted: Font: (Default) Times New Roman

Formatted: Font: (Default) Times New Roman

Formatted: Font: (Default) Times New Roman

Formatted: Font: (Default) Times New Roman

Formatted: Font: (Default) Times New Roman

Formatted: Font: (Default) Times New Roman

Formatted: Font: (Default) Times New Roman

Formatted: Font: (Default) Times New Roman

Formatted: Font: (Default) Times New Roman

Formatted: Font: (Default) Times New Roman

Formatted: Font: (Default) Times New Roman

Formatted: Font: (Default) Times New Roman

Formatted: Font: (Default) Times New Roman

Formatted: Font: (Default) Times New Roman

896 Neumann, K., Elbersen, B. S., Verburg, P. H., Staritsky, I., Pérez-Soba, M., de Vries, W., and Rienks, W.
897 A.: Modelling the spatial distribution of livestock in Europe, *Landscape. Ecol.*, 24, 1207-1222,
898 <https://doi.org/10.1007/s10980-009-9357-5>, 2009.

899 Nicolas, G., Robinson, T. P., Wint, G. R., Conchedda, G., Cinardi, G., and Gilbert, M.: Using Random
900 Forest to Improve the Downscaling of Global Livestock Census Data, *Plos. One.*, 11, e0150424,
901 <https://doi.org/10.1371/journal.pone.0150424>, 2016.

902 O'Neill, D. W. and Abson, D. J.: To settle or protect? A global analysis of net primary production in
903 parks and urban areas, *Ecol. Econ.*, 69, 319-327, <https://doi.org/10.1016/j.ecolecon.2009.08.028>,
904 2009.

905 Pan, Y. J., Chen, S. Y., Qiao, F. X., Ukkusuri, S. V., and Tang, K.: Estimation of real-driving emissions
906 for buses fueled with liquefied natural gas based on gradient boosted regression trees, *Sci. Total
907 Environ.*, 660, 741-750, <https://doi.org/10.1016/j.scitotenv.2019.01.054>, 2019.

908 Petz, K., Alkemade, R., Bakkenes, M., Schulp, C. J. E., van der Velde, M., and Leemans, R.: Mapping
909 and modelling trade-offs and synergies between grazing intensity and ecosystem services in
910 rangelands using global-scale datasets and models, *Global. Environ. Chang.*, 29, 223-234,
911 <https://doi.org/10.1016/j.gloenvcha.2014.08.007>, 2014.

912 Pozo, R. A., Cusack, J. J., Acebes, P., Malo, J. E., Traba, J., Iranzo, E. C., Morris-Trainor, Z.,
913 Minderman, J., Bunnefeld, N., Radic-Schilling, S., Moraga, C. A., Arriagada, R., and Corti, P.:
914 Reconciling livestock production and wild herbivore conservation: challenges and opportunities,
915 *Trends. Ecol. Evol.*, 36, 750-761, <https://doi.org/10.1016/j.tree.2021.05.002>, 2021.

916 Prosser, D. J., Wu, J., Ellis, E. C., Gale, F., Van Boeckel, T. P., Wint, W., Robinson, T., Xiao, X., and
917 Gilbert, M.: Modelling the distribution of chickens, ducks, and geese in China, *Agric Ecosyst
918 Environ.*, 141, 381-389, <https://doi.org/10.1016/j.agee.2011.04.002>, 2011.

919 Robinson, T. P., Wint, G. R., Conchedda, G., Van Boeckel, T. P., Ercoli, V., Palamara, E., Cinardi, G.,
920 D'Aiotti, L., Hay, S. I., and Gilbert, M.: Mapping the global distribution of livestock, *Plos. One.*, 9,
921 e96084, <https://doi.org/10.1371/journal.pone.0096084>, 2014.

922 Rokach, L.: Decision forest: Twenty years of research, *Inform. Fusion.*, 27, 111-125,
923 <https://doi.org/10.1016/j.inffus.2015.06.005>, 2016.

924 Shakoor, A., Shakoor, S., Rehman, A., Ashraf, F., Abdullah, M., Shahzad, S. M., Farooq, T. H., Ashraf,
925 M., Manzoor, M. A., Altaf, M. M., and Altaf, M. A.: Effect of animal manure, crop type, climate
926 zone, and soil attributes on greenhouse gas emissions from agricultural soils-A global meta-analysis,
927 *J. Clean. Prod.*, 278, 124019, <https://doi.org/10.1016/j.jclepro.2020.124019>, 2021.

928 Sun, J., Liu, M., Fu, B. J., Kemp, D., Zhao, W. W., Liu, G. H., Han, G. D., Wilkes, A., Lu, X. Y., Chen,
929 Y. C., Cheng, G. W., Zhou, T. C., Hou, G., Zhan, T. Y., Peng, F., Shang, H., Xu, M., Shi, P. L., He, Y.
930 T., Li, M., Wang, J. N., Tsunekawa, A., Zhou, H. K., Liu, Y., Li, Y. R., and Liu, S. L.: Reconsidering
931 the efficiency of grazing exclusion using fences on the Tibetan Plateau, *Sci. Bull.*, 65, 1405-1414,
932 <https://doi.org/10.1016/j.scib.2020.04.035>, 2020.

933 Sun, Y. X., Liu, S. L., Liu, Y. X., Dong, Y. H., Li, M. Q., An, Y., and Shi, F. N.: Grazing intensity and
934 human activity intensity data sets on the Qinghai - Tibetan Plateau during 1990 - 2015, *Geoscience.
935 Data. Journal.*, 9, 140-153, <https://doi.org/10.1002/gdj3.127>, 2021.

936 Tabassum, A., Abbasi, T., and Abbasi, S. A.: Reducing the global environmental impact of livestock
937 production: the minilivestock option, *J. Clean. Prod.*, 112, 1754-1766,
938 <https://doi.org/10.1016/j.jclepro.2015.02.094>, 2016.

939 Van Boeckel, T. P., Prosser, D., Franceschini, G., Biradar, C., Wint, W., Robinson, T., and Gilbert, M.:

Formatted: Font: (Default) Times New Roman

Formatted: Font: (Default) Times New Roman

Formatted: Font: (Default) Times New Roman

Formatted: Font: (Default) Times New Roman

Formatted: Font: (Default) Times New Roman

Formatted: Font: (Default) Times New Roman

Formatted: Font: (Default) Times New Roman

Formatted: Font: (Default) Times New Roman

Formatted: Font: (Default) Times New Roman

Formatted: Font: (Default) Times New Roman

Formatted: Font: (Default) Times New Roman

Formatted: Font: (Default) Times New Roman

Formatted: Font: (Default) Times New Roman

Formatted: Font: (Default) Times New Roman

Formatted: Font: (Default) Times New Roman

Formatted: Font: (Default) Times New Roman

Formatted: Font: (Default) Times New Roman

Formatted: Font: (Default) Times New Roman

Formatted: Font: (Default) Times New Roman

Formatted: Font: (Default) Times New Roman

Formatted: Font: (Default) Times New Roman

Formatted: Font: (Default) Times New Roman

Formatted: Font: (Default) Times New Roman

Formatted: Font: (Default) Times New Roman

Formatted: Font: (Default) Times New Roman

Formatted: Font: (Default) Times New Roman

940 Modelling the distribution of domestic ducks in Monsoon Asia, *Agr. Ecosyst. Environ.*, 141, 373-380,
941 <https://doi.org/10.1016/j.agee.2011.04.013>, 2011.

942 Veldhuis, M. P., Ritchie, M. E., Ogotu, J. O., Morrison, T. A., Beale, C. M., Estes, A. B., Mwakilema,
943 W., Ojwang, G. O., Parr, C. L., Probert, J., Wargute, P. W., Hopcraft, J. G. C., and Han, O.:
944 Cross-boundary human impacts compromise the Serengeti-Mara ecosystem, *Science.*, 363,
945 1424-1428, <https://doi.org/10.1126/science.aav0564>, 2019.

946 Venglovsky, J., Sasakova, N., and Placha, I.: Pathogens and antibiotic residues in animal manures and
947 hygienic and ecological risks related to subsequent land application, *Bioresour. Technol.*, 100,
948 5386-5391, <https://doi.org/10.1016/j.biortech.2009.03.068>, 2009.

949 Waha, K., van Wijk, M. T., Fritz, S., See, L., Thornton, P. K., Wichern, J., and Herrero, M.: Agricultural
950 diversification as an important strategy for achieving food security in Africa, *Glob. Chang. Biol.*, 24,
951 3390-3400, <https://doi.org/10.1111/gcb.14158>, 2018.

952 Wang, R. J., Feng, Q. S., Jin, Z. R., and Liang, T. G.: The Restoration Potential of the Grasslands on the
953 Tibetan Plateau, *Remote. Sens.*, 14, 80, <https://doi.org/10.3390/rs14010080>, 2021.

954 Wang, Y. F., Lv, W. W., Xue, K., Wang, S. P., Zhang, L. R., Hu, R. H., Zeng, H., Xu, X. L., Li, Y. M.,
955 Jiang, L. L., Hao, Y. B., Du, J. Q., Sun, J. P., Dorji, T., Piao, S. L., Wang, C. H., Luo, C. Y., Zhang, Z.
956 H., Chang, X. F., Zhang, M. M., Hu, Y. G., Wu, T. H., Wang, J. Z., Li, B. W., Liu, P. P., Zhou, Y.,
957 Wang, A., Dong, S. K., Zhang, X. Z., Gao, Q. Z., Zhou, H. K., Shen, M. G., Wilkes, A., Mieke, G.,
958 Zhao, X. Q., and Niu, H. S.: Grassland changes and adaptive management on the Qinghai-Tibetan
959 Plateau, *Nat. Rev. Earth. Env.*, 3, 668-683, <https://doi.org/10.1038/s43017-022-00330-8>, 2022.

960 Wang, Y. X., Sun, Y., Wang, Z. F., Chang, S. H., and Hou, F. J.: Grazing management options for
961 restoration of alpine grasslands on the Qinghai - Tibet Plateau, *Ecosphere.*, 9, e02515,
962 <https://doi.org/10.1002/ecs2.2515>, 2018.

963 Wei, Y. Q., Lu, H. Y., Wang, J. N., Wang, X. F., and Sun, J.: Dual Influence of Climate Change and
964 Anthropogenic Activities on the Spatiotemporal Vegetation Dynamics Over the Qinghai-Tibetan
965 Plateau From 1981 to 2015, *Earth's Future.*, 10, 1-23, <https://doi.org/10.1029/2021EF002566>, 2022.

966 Yang, J. and Huang, X.: The 30 m annual land cover dataset and its dynamics in China from 1990 to
967 2019, *Earth. Syst. Sci. Data.*, 13, 3907-3925, <https://doi.org/10.5194/essd-13-3907-2021>, 2021.

968 Yang, Y. J., Song, G., and Lu, S.: Assessment of land ecosystem health with Monte Carlo simulation: A
969 case study in Qiqihaer, China, *J. Clean. Prod.*, 250, 119522, 2020.

970 Ye, T., Liu, W. H., Mu, Q. Y., Zong, S., Li, Y. J., and Shi, P. J.: Quantifying livestock vulnerability to
971 snow disasters in the Tibetan Plateau: Comparing different modeling techniques for prediction,
972 *International Journal of Disaster Risk Reduction*, 48, <https://doi.org/10.1016/j.ijdrr.2020.101578>,
973 2020.

974 Zhai, D. C., Gao, X. Z., Li, B. L., Yuan, Y. C., Jiang, Y. H., Liu, Y., Li, Y., Li, R., Liu, W., and Xu, J.:
975 Driving Climatic Factors at Critical Plant Developmental Stages for Qinghai-Tibet Plateau Alpine
976 Grassland Productivity, *Remote. Sens.*, 14, 1564, <https://doi.org/10.3390/rs14071564>, 2022.

977 Zhan, N., Liu, W. H., Ye, T., Li, H. D., Chen, S., and Ma, H.: High-resolution livestock seasonal
978 distribution data on the Qinghai-Tibet Plateau in 2020, *Sci. Data.*, 10, 142,
979 <https://doi.org/10.1038/s41597-023-02050-0>, 2023.

980 Zhang, B. H., Zhang, Y. L., Wang, Z. F., Ding, M. J., Liu, L. S., Li, L. H., Li, S. C., Liu, Q. H., Paudel,
981 B., and Zhang, H. M.: Factors Driving Changes in Vegetation in Mt. Qomolangma (Everest):
982 Implications for the Management of Protected Areas, *Remote. Sens.*, 13, 4725,
983 <https://doi.org/10.3390/rs13224725>, 2021a.

Formatted: Font: (Default) Times New Roman

Formatted: Font: (Default) Times New Roman

Formatted: Font: (Default) Times New Roman

Formatted: Font: (Default) Times New Roman

Formatted: Font: (Default) Times New Roman

Formatted: Font: (Default) Times New Roman

Formatted: Font: (Default) Times New Roman

Formatted: Font: (Default) Times New Roman

Formatted: Font: (Default) Times New Roman

Formatted: Font: (Default) Times New Roman

Formatted: Font: (Default) Times New Roman

Formatted: Font: (Default) Times New Roman

Formatted: Font: (Default) Times New Roman

Formatted: Font: (Default) Times New Roman

Formatted: Font: (Default) Times New Roman

Formatted: Font: (Default) Times New Roman

Formatted: Font: (Default) Times New Roman

Formatted: Font: (Default) Times New Roman

Formatted: Font: (Default) Times New Roman

Formatted: Font: (Default) Times New Roman

Formatted: Font: (Default) Times New Roman

Formatted: Font: (Default) Times New Roman

Formatted: Font: (Default) Times New Roman

Formatted: Font: (Default) Times New Roman

Formatted: Font: (Default) Times New Roman

Formatted: Font: (Default) Times New Roman

984 Zhang, R. Y., Wang, Z. W., Han, G. D., Schellenberg, M. P., Wu, Q., and Gu, C.: Grazing induced
985 changes in plant diversity is a critical factor controlling grassland productivity in the Desert Steppe,
986 Northern China, *Agr. Ecosyst. Environ.*, 265, 73-83, <https://doi.org/10.1016/j.agee.2018.05.014>,
987 2018.

988 Zhang, W. B., Li, J., Struik, P. C., Jin, K., Ji, B. M., Jiang, S. Y., Zhang, Y., Li, Y. H., Yang, X. J., and
989 Wang, Z.: Recovery through proper grazing exclusion promotes the carbon cycle and increases
990 carbon sequestration in semiarid steppe, *Sci. Total. Environ.*, 892, 164423,
991 <https://doi.org/10.1016/j.scitotenv.2023.164423>, 2023.

992 Zhang, Y., Hu, Q. W., and Zou, F. L.: Spatio-Temporal Changes of Vegetation Net Primary Productivity
993 and Its Driving Factors on the Qinghai-Tibetan Plateau from 2001 to 2017, *Remote. Sens.*, 13, 1566,
994 <https://doi.org/10.3390/rs13081566>, 2021b.

995 Zhao, X. Q., Xu, T. W., Ellis, J., He, F. Q., Hu, L. Y., and Li, Q.: Rewilding the wildlife in
996 Sangjiangyuan National Park, Qinghai-Tibetan Plateau, *Ecosyst. Health. Sust.*, 6, 1776643,
997 <https://doi.org/10.1080/20964129.2020.1776643>, 2020.

998 Zhou, W. X., Li, C. J., Wang, S., Ren, Z. B., and Stringer, L. C.: Effects of grazing and enclosure
999 management on soil physical and chemical properties vary with aridity in China's drylands, *Sci.*
1000 *Total. Environ.*, 877, 162946, <https://doi.org/10.1016/j.scitotenv.2023.162946>, 2023.

1001 Zhu, Q., Chen, H., Peng, C. H., Liu, J. X., Piao, S., He, J. S., Wang, S. P., Zhao, X. Q., Zhang, J., Fang,
1002 X. Q., Jin, J. X., Yang, Q. E., Ren, L. L., and Wang, Y. F.: An early warning signal for grassland
1003 degradation on the Qinghai-Tibetan Plateau, *Nat. Commun.*, 14, 6406,
1004 <https://doi.org/10.1038/s41467-023-42099-4>, 2023a.

1005 Zhu, Y. Y., Zhang, H. M., Ding, M. J., Li, L. H., and Zhang, Y. L.: The Multiple Perspective Response
1006 of Vegetation to Drought on the Qinghai-Tibetan Plateau, *Remote. Sens.*, 15, 902,
1007 <https://doi.org/10.3390/rs15040902>, 2023b.

1008 [Zhou, J., Niu, J., Wu, N., Lu, T. Annual high-resolution grazing intensity maps on the Qinghai-Tibet](#)
1009 [Plateau from 1990 to 2020 \[Dataset\]. Zenodo.](#)
1010 <https://doi.org/10.5281/zenodo.13141090><https://doi.org/10.5281/zenodo.1085119>, 2024.

1011

Formatted: Font: (Default) Times New Roman

Formatted: Font: (Default) Times New Roman

Formatted: Font: (Default) Times New Roman

Formatted: Font: (Default) Times New Roman

Formatted: Font: (Default) Times New Roman

Formatted: Font: (Default) Times New Roman

Formatted: Font: (Default) Times New Roman

Formatted: Font: (Default) Times New Roman

Formatted: Font: (Default) Times New Roman

Formatted: Font: (Default) Times New Roman

Formatted: Font: (Default) Times New Roman

Formatted: Font: (Default) Times New Roman

Formatted: Font: (Default) Times New Roman

Formatted: Font: (Default) Times New Roman